A phospholipase B from *Pseudomonas aeruginosa* with activity towards endogenous phospholipids affects biofilm assembly

Andrea J. Weiler[1], Olivia Spitz[2], Mirja Gudzuhn[3], Stephan N. Schott-Verdugo[4,5,7], Michael Kamel[6], Björn Thiele[8], Wolfgang R. Streit[3], Alexej Kedrov[6], Lutz Schmitt[2], Holger Gohlke[4,7] and Filip Kovacic[1,*]

1. Institute of Molecular Enzyme Technology, Heinrich Heine University Düsseldorf, Forschungszentrum Jülich GmbH, D-52425 Jülich, Germany
2. Institute of Biochemistry, Heinrich-Heine-University Düsseldorf, 40225 Düsseldorf, Germany
3. Department of Microbiology and Biotechnology, University of Hamburg, Ohnhorststr. 18, 22609 Hamburg, Germany
4. Institute for Pharmaceutical and Medicinal Chemistry, Heinrich Heine University Düsseldorf, 40225 Düsseldorf, Germany
5. Centro de Bioinformática y Simulación Molecular (CBSM), Facultad de Ingeniería, Universidad de Talca, 2 Norte 685, CL-3460000 Talca, Chile
6. Synthetic Membrane Systems, Institute of Biochemistry, Heinrich Heine University Düsseldorf, 40225 Düsseldorf, Germany
7. John von Neumann Institute for Computing (NIC), Jülich Supercomputing Centre (JSC), Institute of Biological Information Processing (IBI-7: Structural Biochemistry) & Institute of Bio- and Geosciences (IBG-4: Bioinformatics), Forschungszentrum Jülich GmbH, 52425 Jülich, Germany
8. Institute of Bio- and Geosciences, Plant Sciences (IBG-2) and Agrosphere (IBG-3), Forschungszentrum Jülich GmbH, D-52425 Jülich, Germany

* Corresponding author: f.kovacic@fz-juelich.de

Keywords: oligomerization, virulence factor, membrane protein, α/β-hydrolase, pathogen

Abstract

Pseudomonas aeruginosa is a severe threat to immunocompromised patients due to its numerous virulence factors and biofilm-mediated multidrug resistance. It produces and secretes various toxins with hydrolytic activities including phospholipases. However, the function of intracellular phospholipases for bacterial virulence has still not been established. Here, we demonstrate that the hypothetical gene *pa2927* of *P. aeruginosa* encodes a novel phospholipase B named PaPlaB. At reaction equilibrium, PaPlaB purified from detergent-solubilized membranes of *E. coli* released fatty acids (FAs) from *sn*-1 and *sn*-2 positions of phospholipids at the molar ratio of 51:49. PaPlaB *in vitro* hydrolyzed *P. aeruginosa* phospholipids reconstituted in detergent micelles and phospholipids reconstituted in vesicles. Cellular localization studies indicate that PaPlaB is a cell-bound PLA of *P. aeruginosa* and that it is peripherally bound to both membranes in *E. coli*, yet the active form was predominantly associated with the cytoplasmic membrane of *E. coli*. Decreasing the concentration of purified and detergent-stabilized PaPlaB leads to increased enzymatic activity, and at the same time triggers oligomer dissociation. We showed that the free FA profile, biofilm amount and architecture of the wild type and Δ*plaB* differ. However, it remains to be established how the PLB activity of PaPlaB is regulated by homooligomerisation and how it relates to the phenotype of the *P. aeruginosa* Δ*plaB*. This novel putative virulence factor contributes to our understanding of phospholipid degrading enzymes and might provide a target for new therapeutics against *P. aeruginosa* biofilms.

1. Introduction

P. aeruginosa causes severe hospital-associated infections, especially in immunocompromised hosts, which are complicated to treat due to the increasing antibiotic resistance and the aggressive nature of this pathogen leading to the fast progression of the infection [1, 2]. In general, the overall mortality rate determined on a large group of 213,553 patients with *P. aeruginosa* septicemia was 16 %, going along with the observation that the incidence of sepsis has increased since 2001 [3]. This clearly illustrates a need for novel treatments to kill the pathogen or, at least, diminish its virulence. Therefore, the World Health Organization has classified *P. aeruginosa*, together with other "ESKAPE" pathogens including *Enterobacter faecium*, *Staphylococcus aureus*, *Klebsiella pneumoniae*, *Acinetobacter baumannii*, and *Enterobacter spp*., in a priority group for research and development of novel antibiotics. Unfortunately, despite intensive investigations towards understanding the virulence of *P. aeruginosa*, many genes encoding putative virulence factors remain uncharacterized [4].

In *P. aeruginosa*, as well as in other bacterial pathogens, phospholipases, hydrolases with membrane phospholipid-degrading activity, play an important role during infections [5, 6]. They are classified into several groups depending on which ester bond of a glycerophospholipid (GPL) they hydrolyze [7]. While phospholipases C (PLC) and D (PLD), respectively, hydrolyze the glycerol-oriented and the head group-oriented phosphodiester bonds of phospholipids, phospholipases A1 (PLA1) and A2 (PLA2) release fatty acids bound at the *sn*-1 or *sn*-2 positions, respectively. Phospholipases B (PLB) cleave *sn*-1 and *sn*-2 bonds of GPL with similar specificity. Lysophospholipids, degradation products of PLA1 and PLA2, are converted by lysophospholipases A (lysoPLA) to a glycerophosphoalcohol and a fatty acid.

The contribution of bacterial phospholipases to virulence is predominantly related to damaging the host cells, which mostly enhances the survival and spread of the pathogen in the host [5, 6]. Several

phospholipases of *P. aeruginosa*, namely phospholipases A, ExoU [8] and PlaF [9, 10], phospholipase A EstA [11], phospholipase C PlcH [12], and two phospholipases D, PldA and PldB [13], were suggested to be virulence factors in that way. The type III secreted ExoU, and type VI secreted PldA and PldB are directly delivered into eukaryotic cells, where they modulate native host pathways to facilitate invasion by *P. aeruginosa* or inflammation [14]. An EstA of *P. aeruginosa,* which is anchored to the outer membrane with the catalytic domain protruding into the extracellular medium, was shown to affects virulence- and resistance-related phenotypes (cell motility and biofilm formation) [11]. PlcH, one of three secreted PLCs of *P. aeruginosa*, is considered as a virulence factor because (i) it exhibits hemolytic activity; (ii) it is produced during clinical infection with *P. aeruginosa* [15], and (iii) *plcH* deletion strain of *P. aeruginosa* shows attenuated virulence in mouse burn models [16]. However, despite more than three decades of research on phospholipases, still little is known about the direct action of *P. aeruginosa* phospholipases on the bacterial membrane.

On the contrary, one of the best-studied pathogens concerning phospholipases is *Legionella pneumophila,* an intracellularly replicating Gram-negative bacterium [17]. Several phospholipases of *L. pneumophila* were proposed to have a function for establishing a proper life cycle inside a host. One of them is the major surface-associated phospholipase PlaB (LpPlaB). LpPlaB is a serine hydrolase with hemolytic activity and catalytic activity towards common bacterial phospholipids and lysophospholipids containing glycerol and choline head groups [18, 19]. However, the catalytic mechanism of LpPlaB, the mechanism of targeting to the outer membrane, structural features responsible for binding to the membrane, and its effect on the host are unknown.

Here, we expressed, purified, and characterized a homolog of LpPlaB from the human pathogen *P. aeruginosa* PA01, which we named PaPlaB. Comprehensive phospholipolytic enzyme activity studies revealed that PaPlaB is a promiscuous PLB and lysoPLA, which shows strong activity towards endogenous phospholipids isolated from *P. aeruginosa*. Furthermore, we demonstrated that a

P. aeruginosa Δ*plaB* deletion strain produces less biofilm with a different architecture compared to the wild-type bacterium. Thus, the PaPlaB is a novel putative virulence factor of *P. aeruginosa* PA01 belonging to the poorly understood PLB family.

2. Material and methods

2.1 Sequence analysis

Amino acid sequence search and alignment were performed using BLAST and alignment tools provided by the National Center for Biotechnology Information (www.ncbi.nlm.nih.gov) [20]. The sequence alignment was visualized using BioEdit software [21]. TMpred server (https://embnet.vital-it.ch/software/TMPRED_form.html) was used to predict transmembrane helices with the length between 17 and 33 residues. Putative TM helices have TMpred scores above 500.

2.2 Molecular cloning

The *paplaB* gene containing the sequence that encodes a C-terminal His_6-tag was amplified using Phusion® DNA polymerase (Thermo Fisher Scientific, Darmstadt, Germany). In the PCR, the genomic DNA of *P. aeruginosa* PA01 [22], isolated with the DNeasy blood and tissue kit (QIAGEN, Germany), was used as the template together with primers paplaB_for and paplaB_rev (Table S1). The pET22-*paplaB* vector for T7 RNA polymerase-controlled expression of *paplaB* was constructed by ligation of the *paplaB* gene into the pET22b vector (Novagen, Germany) at *Nde*I and *Sac*I restriction sites, using T4 DNA ligase (Thermo Fisher Scientific). Site-directed mutagenesis of PaPlaB was performed by the Quick® Change PCR method using the pET22-*paplaB* plasmid as a template and complementary mutagenic oligonucleotide pairs (Table S1) [23]. *E. coli* DH5α strain [24] was used for molecular cloning experiments. After electrophoresis, the plasmid DNA and DNA fragments from the agarose gel (1 % w/v) were isolated with innuPREP Plasmid Mini Kit 2.0 and the innuPREP

DOUBLEpure Kit (Analytik Jena, Germany), respectively. Oligonucleotides synthesis and plasmid DNA sequencing was performed by Eurofins Genomics (Germany).

2.3 Protein expression and purification

For the expression of PaPlaB with a C-terminal His_6-tag, *E. coli* C43(DE3) [25] cells were transformed with pET22-*paplaB* plasmid, and the empty pET22b vector was used as a control. Cells were grown overnight in lysogeny broth (LB) medium [26] supplemented with ampicillin (100 µg/ml) at 37°C with agitation. Overnight cultures were used to inoculate the expression cultures to an initial OD_{580nm} = 0.05 in LB medium containing ampicillin (100 µg/ml). The cultures were grown at 37°C, and the expression of *paplaB* was induced with isopropyl-β-D-thiogalactoside (IPTG, 1 mM) at OD_{580nm} = 0.4 - 0.6 followed by incubation at 37°C for 5 hours. The cells were harvested by centrifugation (6,000 *g*, 4°C, 10 min) and stored at -20° C before further analysis. Active site variants of PaPlaB carrying S79A, D196A, or H244A mutations were expressed the same way as PaPlaB.

Cells producing PaPlaB were suspended in 100 mM Tris-HCl pH 8, disrupted by a French press, and incubated for 30 min with lysozyme (2 mg/ml) and DNase (0.5 mg/ml). The cell debris and inclusion bodies were removed by centrifugation (6,000 *g*, 4°C, 10 min), and the soluble cell lysate was ultracentrifuged (180,000 *g*, 4°C, 2 h) to isolate the membrane fraction. Subsequently, the proteins were extracted from the membranes upon overnight incubation in the solubilization buffer (5 mM Tris-HCl pH 8, 300 mM NaCl; 50 mM KH_2PO_4; 20 mM imidazole, Triton X-100 1 % v/v) at 4°C. Insoluble debris was removed by ultracentrifugation (180,000 *g*, 4°C, 0.5 h), and the supernatant containing PaPlaB was used for purification.

Immobilized metal affinity chromatographic purification of PaPlaB was performed [27] using the ÄKTA Pure instrument (GE Healthcare). The Ni^{2+}-NTA column (4 ml; Macherey-Nagel, Düren) was equilibrated with ten column volumes of the solubilization buffer before loading the sample. The column was washed with five column volumes of the washing buffer (5 mM Tris-HCl pH 8, 300 mM

NaCl, 50 mM KH_2PO_4, 50 mM imidazole, 0.22 mM DDM) to remove unspecifically bound proteins followed by the elution of PaPlaB with 100 ml of buffer (5 mM Tris-HCl pH 8, 300 mM NaCl, 50 mM KH_2PO_4, 0.22 mM DDM) in which the concentration of imidazole was increased linearly from 50 to 500 mM. The fractions containing pure PaPlaB were transferred into 100 mM Tris-HCl, pH 8 supplemented with 0.22 mM DDM by gel filtration using the PD-10 column (GE Healthcare). Samples were concentrated using an Amicon®Ultra-4 ultrafiltration device, with a cut-off of 10 kDa (Merck Millipore). The protein was incubated at 4°C for 1 h with Bio-Beads™ SM-2 resin (Bio-Rad) equilibrated with 100 mM Tris-HCl, pH 8 to remove excess detergent.

2.4 *In vitro* separation of inner and outer membranes

The separation of the inner and outer membranes of *E. coli* C43(DE3) pET22-*paplaB* (25 ml LB medium, 37°C, 5 h after induction) was performed with a continuous sucrose gradient (20 - 70 % w/v in 100 mM Tris-HCl pH 7.4). The gradients were prepared in SW40-type tubes (Beckman Coulter) using the Gradient Station (Biocomp Instruments, Canada). Isolated membranes were suspended in buffer containing 20 % (w/v) sucrose and loaded on the top of the continuous sucrose gradient followed by ultracentrifugation at 110,000 *g* for 16 h, 4°C in swinging-bucket rotor SW40 (Beckman Coulter). Fractions (1 ml) were collected from the top using the Gradient Station equipped with a TRIAX UV-Vis flow-cell spectrophotometer (Biocomp Instruments, Canada). The sucrose concentration in collected fractions was determined with a refractometer (OPTEC, Optimal Technology, Baldock UK).

2.5 Separation of integral and peripheral bound protein

To identify whether PaPlaB is an integrally or peripherally bound protein, membranes were isolated from *E. coli* C43(DE3) pET22b-*paplaB* expression culture (100 ml). The isolated membranes were suspended in 500 µl of the following buffers: MES buffer as negative control (20 mM, pH 6.5), an aqueous solution of Na_2CO_3 (10 mM), urea (4 M) in MES buffer (20 mM, pH 6.5), Triton X-100 (2%

v/w) in MES buffer (20 mM, pH 6.5). Membranes were incubated at 22 °C for one hour followed by ultracentrifugation at 20,000 *g* for 2 h, 4°C in rotor 55.2 Ti (Beckmann Coulter, California, USA).

2.6 SDS-PAGE and immunodetection

The sodium dodecyl sulfate-polyacrylamide gel electrophoresis (SDS-PAGE) was performed according to the method of Laemmli [28], and the gels were stained with Coomassie Brilliant Blue G-250. For immunodetection of PaPlaB, the gel was loaded with 10 µl of the cell, soluble and membrane fractions isolated from the cell suspension with OD_{580nm} = 25. After SDS-PAGE, proteins were transferred from the gel onto a polyvinylidene difluoride membrane [29] and detected with the anti-His (C-terminal)-HRP antibody (Thermo Fisher/Invitrogen) according to the manufacturer's instructions. The concentration of PaPlaB was determined using the UV-VIS spectrophotometer NanoDrop 2000c (Thermo Fisher Scientific). The extinction coefficient ε = 73.005 M^{-1} cm^{-1} was calculated with the ProtParam tool [30].

2.7 Enzyme activity assay and inhibition

Esterase activity of PaPlaB was determined in a 96-well microtiter plate (MTP) at 37°C by combining 10 µl of enzyme sample with 150 µl of the *p*-nitrophenyl butyrate (*p*-NPB) substrate [7]. Hydrolytic activities towards glycerophospholipids (GPLs) and lysoGPLs (Table S2), which were purchased from Avanti Polar lipids (Alabaster, USA), were determined by quantification of released fatty acids using NEFA assay kit (Wako Chemicals, Neuss, Germany) [7]. Lipids were dissolved in NEFA buffer (50 mM Tris, 100 mM NaCl, 1 mM $CaCl_2$, 1 % (v/v) Triton X-100, pH 7.2). Small unilamellar vesicles (SUVs, 3.3 mg/ml) for enzyme assay were prepared using 1,2-dioleoyl-sn-glycero-3-phospho-(1'-rac-glycerol) (DOPG) and 1,2-dioleoyl-sn-glycero-3-phosphoethanolamine (DOPE) at molar ratio 75 : 20 as described previously [31]. The enzymatic reactions were performed by combining 12.5 µl of enzyme sample with 12.5 µl of a lipid substrate (0.67 mM) at 37°C for 15 min. The enzymatic reactions with SUVs made of DOPE:DOPG were performed by combining 100 µl of enzyme sample with 100 µl of

SUV (3.3 mg/ml) at 37°C for 4h. Prior incubation of PaPlaB with SUVs detergent was removed by incubating 500 µl PaPlaB with 20 BioBeads SM-2 (Bio Rad, Munick, Germany) for 30 min at room temperature. The fatty acid amount was calculated from the calibration curve made with 0.5, 1, 2, 3, 4, and 5 nmol oleic acid.

The inhibition of PaPlaB with PMSF, paraoxon (both were dissolved in propane-2-ol), and EDTA (dissolved in 100 mM Tris-HCl pH 8) was tested as described previously [9]. Inhibition of PaPlaB was performed by incubating enzyme aliquots with the inhibitors for 1.5 h at 30°C, followed by a determination of the enzymatic activity using the *p*-NPB substrate.

2.8 Gas chromatography-mass spectrometric (GC-MS) phospholipase B activity assay

FAs were extracted after 1 h incubation (37°C) of purified PaPlaB (2 ml, 4.28 µg/ml) with 1-oleoyl-2-palmitoyl-PC ($PC_{18:1\text{-}16:0}$; 0.5 mM) in 2 ml NEFA buffer. After incubation, 1 ml of NEFA buffer was added, and FAs were extracted with 12 ml $CHCl_3$: CH_3OH = 2 : 1. The upper chloroform phase was withdrawn, and FAs were extracted again with 8 ml $CHCl_3$. $CHCl_3$ extracts were combined, and $CHCl_3$ was evaporated. FAs were extracted from cells suspended in 20 ml H_2O the same way as described for FA extraction from the supernatant.

FAs were dissolved in 200 µl $CHCl_3$. The $CHCl_3$ extract was mixed with ten volumes of acetonitrile and filtered through a 0.2 µm pore size filter. The residues of the PaPlaB extracts were dissolved in 1 ml acetonitrile : methylenchloride = 4 : 1. Before GC-MS analysis, FAs acids in the PaPlaB extracts and standard solutions were derivatized to trimethylsilylesters. For this purpose, 100 µl of each sample solution was mixed with 700 µl acetonitrile, 100 µl pyridine and 100 µl N-methyl-N-(trimethylsilyl) trifluoroacetamide and heated to 90°C for 1 h. An acetonitrile solution of FAs mixture containing 1 mM $C_{10:0}$, $C_{12:0}$, $C_{14:0}$-, $C_{16:0}$, $C_{18:0}$ and $C_{18:1}$ (oleic acid) was diluted to 50, 100, 200 and 400 µM and derivatized in the same manner as above. The GC-MS system consisted of an Agilent gas chromatograph 7890A and autosampler G4513A (Agilent, CA, USA) coupled to a TOF mass

spectrometer JMS-T100GCV AccuTOF GCv (Jeol, Tokyo, Japan). Analytes were separated on a Zebron-5-HT Inferno column (30 m x 0.25 mm i.d., 0.25 µm film thickness, Phenomenex, USA). Helium was used as carrier gas at a constant gas flow of 1.0 ml/min. The oven temperature program employed for analysis of silylated fatty acids was as follows: 80°C; 5°C/min to 300°C, held for 1 min. The injector temperature was held at 300°C, and all injections (1 µl) were made in the split mode (1:10). The mass spectrometer was used in the electron impact (EI) mode at an ionizing voltage of 70 V and an ionizing current of 300 µA. Analytes were scanned over the range m/z 50 - 750 with a spectrum recording interval of 0.4 s. The GC interface and ion chamber temperature were both kept at 250°C. After the conversion of the raw data files to the cdf-file format, data processing was performed by the use of the software XCalibur 2.0.7 (ThermoFisher Scientific). Fatty acids from the PaPlaB sample were identified by comparison of their retention times and mass spectra with those of fatty acid standards.

2.9 Gas chromatography-mass spectrometric (GC-MS) analysis of FAs extracted from cells

Cells from *P. aeruginosa* PA01 and Δ*plaB* overnight cultures (37˚C, 25 ml LB medium, agitation) were harvested (10 min, 2790×*g*, room temperature) and the supernatant was filtered through a filter with 0.2 µm pore size to remove residual cells. FAs were extracted from supernatant (20 ml) with $CHCl_3$: CH_3OH = 2 : 1 (60 ml). The upper chloroform phase was withdrawn, and FAs were extracted again with 40 ml $CHCl_3$. Chloroform extracts were combined and chloroform was evaporated. FAs were extracted from cells suspended in 20 ml H_2O as described for supernatant.

FAs were transferred to 15 ml Falcon tubes by dissolving in 500 µL CH_2Cl_2 twice. After evaporation to dryness, the remaining fatty acids were derivatized to methyl esters according to Funada et al. with modifications.[32] Briefly, the residues were dissolved in 1 ml sulfuric acid (1 M) in methanol and incubated in an ultrasonic bath for 30 min. The fatty acid methyl esters (FAMEs) were extracted after the addition of 3.3 ml H_2O and 1.7 ml hexane by vigorous shaking for 1 min. The upper organic

phase was withdrawn and dried over sodium carbonate. An aliquote was directly used for GC-MS analysis. A methanol solution of FAs containing 1 mM of $C_{10:0}$, $C_{12:0}$, $C_{14:0}$, $C_{16:0}$, $C_{18:0}$, $C_{17:0}$ (cyc (9,10)), $C_{18:1}$ (cis-Δ9) and $C_{18:1}$ (trans-Δ11) was diluted to 50, 100, 200 and 400 µM and derivatized the same as described above. The Agilent GC-MS system consisted of a gas chromatograph 7890A and an autosampler G4513A coupled to a quadrupole mass spectrometer MS G3172A (Agilent, CA, USA). Analytes were separated on a SGE^{TM} BPX70 column (30 m x 0.32 mm i.d., 0.25 µm film thickness, Thermo Fisher Scientific, USA). Helium was used as carrier gas at a constant gas flow of 1.5 ml/min. The oven temperature program employed for analysis of FAMEs was as follows: 120°C; 20°C/min to 160°C; 3°C/min to 200°C; 20°C to 220°C, held for 8.7 min. The injector temperature was held at 250°C, and all injections (1 µl) were made in the split mode (1:10). The mass spectrometer was used in the electron impact (EI) mode at an ionizing voltage of 70 eV. Analytes were scanned over the range m/z 50 - 400 with a spectrum recording interval of 4 scans/sec. The GC interface temperature was held at 250°C. The MS source and quadrupole temperatures were kept at 280°C and 150°C, respectively. Data processing was performed by use of the software ChemStation E.02.02.1431 (Agilent, CA, USA). Fatty acids from PlaB samples were identified by comparison of their retention times and mass spectra with those of fatty acid standards and published data. [33-35] Quantification of FAMEs C16:0 (1), C17:0 cyc(9,10) (4), C18:0 (5) and C18:1 trans-Δ^{11} (6) (Fig. 1) were performed by external calibration with the corresponding reference compounds. C18:1 cis-Δ^{11} (7) was quantified by use of the calibration curve of oleic acid (C18:1 cis-Δ^{9}) justified by the almost congruent calibration curves of elaidic acid (C18:1 trans-Δ^{9}) and C18:1 trans-Δ^{11}.

2.10 Thermal stability analysis

Differential scanning fluorimetric analysis of PaPlaB thermal stability was performed using the Prometheus NT.48 nanoDSF instrument (NanoTemper Technologies, Germany) [36]. The Prometheus NT.Plex nanoDSF Grade Standard Capillary Chip containing 10 µl PaPlaB sample per

capillary was heated from 20°C to 90°C at the rate of 0.1°C/min, and the intrinsic fluorescence at wavelengths of 330 nm and 350 nm was measured. The first derivative of the ratio of fluorescence intensities at 350 nm and 330 nm as a function of temperature was used to visualize the denaturing transition and determine the "melting" temperature. Enzyme activity-based thermal stability experiments were performed by measuring the residual esterase activity of a PaPlaB sample incubated 1 h at temperatures from 30°C to 70°C [37]. After the incubation, the enzymatic assay was performed as described above using the *p*-NPB substrate, and the inactivation temperature was determined.

2.11 Multi-angle and dynamic light scattering

Superdex 200 Increase 10/300 GL column (GE Healthcare) was equilibrated overnight at a flow rate of 0.6 ml/min with 100 mM Tris pH 8 containing 0.22 mM DDM. For each multi-angle light scattering (MALS) analysis 200 µl PaPlaB at concentrations of 1, 0.5 and 0.1 mg/ml were loaded to the column at the flow rate of 0.6 ml/min using 1260 binary pump (Agilent Technologies), and the scattered light (miniDAWN TREOS II light scatterer, Wyatt Technologies) and the refractive index (Optilab T-rEX refractometer, Wyatt Technologies) were measured. Data analysis was performed with the software ASTRA 7.1.2.5 (Wyatt Technologies) under the assumption that dn/dc of DDM is 0.1435 ml/g and the extinction coefficient of PaPlaB is 1.450 ml/(mg*cm) [38].

Mean diameters of SUVs were determined using SpectroSize 300 dynamic light scattering (DLS) device (Fa. Xtal Concepts, Hamburg). The measurements (25 times, each 20 s) were performed using a 15 µl sample at 20̊C. The viscosity of water of 1.006 cP was used for calculations.

2.12 Size-exclusion chromatography

Size-exclusion chromatographic (SEC) analysis of PaPlaB in Tris-HCl (100 mM, pH 8, 0.22 mM DDM) buffer was performed using Biosep-SEC-S3000 column (Phenomenex, Aschaffenburg, Germany), LC-10Ai isocratic pump (Shimadzu, Duisburg, Germany), and SPD-M20A photodiode array detector

(Shimadzu, Duisburg, Germany). The molecular weight (M_w) of standard proteins dissolved in the same buffer as PaPlaB was determined (Table S3). For the analysis, 100 µl of PaPlaB or protein standard sample was loaded on the column, and separation was achieved at a flow rate of 0.5 ml/min and 26^{o}C.

2.13 Fluorescence imaging of biofilm in flow chambers

P. aeruginosa PAO1 and Δ*plaB* biofilms were grown on a microscope cover glass (24 mm x 50 mm, thickness 0.17 mm, Carl Roth GmbH & Co. KG, Karlsruhe, Germany), which was fixed with PRESIDENT The Original light body silicon (Coltène/Whaledent AG, Altstätten, Switzerland) on the upper side of the three-channel flow chambers [39]. The flow chambers and tubes (standard tubing, ID 0.8 mm, 1/16" and Tygon Standard R-3607, ID 1.02 mm; Cole-Parmer GmbH, Wertheim, Germany) were sterilized by flushing with sterile chlorine dioxide spray (Crystel TITANIUM, Tristel Solutions Ltd., Snailwell, Cambridgeshire, United Kingdom). Afterward, the flow chambers were filled with 1 % (v/v) sodium hypochlorite, and the tubes were autoclaved. All biofilm experiments were performed at 37°C with a ten-fold diluted LB medium. Before inoculation, the flow chamber was flushed with 1:10 diluted LB medium for 30 minutes with a flow rate of 100 µl/min using the IPC12 High Precision Multichannel Dispenser (Cole-Parmer GmbH, Wertheim, Germany). For inoculation, an overnight culture of *P. aeruginosa* PAO1 or Δ*plaB* was adjusted to an OD_{580nm} of 0.5 in 1:10 diluted LB medium. The diluted culture (300 µl) was inoculated in each channel. After the interruption of medium supply for 1 h, the flow (50 µl/min) was resumed, and the biofilm structure was analyzed after 24, 72, and 144 h grown at 37°C. For visualization, the cells were stained with propidium iodide and SYTO 9 dyes using the LIVE/DEAD™ BacLight™ Bacterial Viability Kit (Thermo Fisher Scientific). Imaging of biofilm was performed using the confocal laser scanning microscope (CLSM) Axio Observer.Z1/7 LSM 800 with Airyscan (Carl Zeiss Microscopy GmbH, Germany) with the objective C-Apochromat 63x/1.20W Korr UV VisIR. The microscope settings for the different fluorescent dyes are shown in Table S4. The

CLSM images and three-dimensional reconstructions were analysed with the ZEN software (version 2.3, Carl Zeiss Microscopy GmbH, Germany). Experiments were repeated two times, each with one biological replicate that was analyzed at three different points by imaging a section of 100 x 100 µm.

2.14 Construction of *P. aeruginosa* Δ*plaB* strain

The *P. aeruginosa* Δ*plaB* mutant strain was generated by homologous recombination [40]. In short, *P. aeruginosa* PAO1 cells were conjugated with the pEMG-*ΔplaB* mutagenesis vector containing the 814 bp fragment of the upstream region of *paplaB*, followed by a gentamicin resistance gene and the 584 bp downstream region of *paplaB*. For that, *E. coli* S17-1 λpir transformed with the pEMG-*ΔplaB* plasmid was used as a donor strain. *Pseudomonas* cells with pEMG-*ΔplaB* plasmid integrated on the chromosome were selected on LB-agar plates containing gentamicin (30 µg/ml), kanamycin (300 µg/ml; a kanamycin resistance gene is encoded on pEMG plasmid) and irgasan (25 µg/ml; used for negative selection of *E. coli*). Cells transformed with the plasmid pSW-2 containing the I-*Sce*I restriction endonuclease were cultivated on LB agar plates containing benzoic acid (2mM; for induction of I-SceI expression) and irgasan (25 µg/ml). The deletion of the *paplaB* gene was confirmed by PCR amplification using the genomic DNA of *P. aeruginosa ΔplaB* as the template (Fig. S1).

2.15 Crystal violet biofilm assay

P. aeruginosa wild-type and Δ*plaB* cultures incubated in LB medium overnight at 37°C in Erlenmeyer flasks (agitation at 150 rpm) were used to inoculate 100 µl culture with OD_{580nm} 0.1 in plastic 96-well MTP. Cultures were grown at 37°C without agitation, and the cells attached to the surface of MTP after removing the planktonic cells were stained with 0.1 % (w/v) crystal violet solution for 15 min, solubilized with acetic acid (30 % v/v) and quantified spectrophotometrically [41].

3. Results

3.1 Expression of *paplaB* in *E. coli* yields a membrane-bound phospholipase A

P. aeruginosa gene *pa2927* encodes a 49.5 kDa protein that shows moderate sequence similarity (39 %) to LpPlaB (Fig. S2), a major cell-associated PLA of *L. pneumophila* [18, 19, 42-46]. We named the *P. aeruginosa* homolog PaPlaB and set out to experimentally test its sequence-based predicted PLA function. To achieve this, we constructed the PaPlaB expression vector (pET22-*paplaB*) suitable for heterologous expression in *E. coli* strains containing the T7 RNA polymerase gene. *PaplaB* gene in pET22-*paplaB* plasmid was modified by including a sequence coding for six histidine residues at the 3' end to enable purification of the protein using immobilized metal affinity chromatography (IMAC). The protein expression was conducted in *E. coli* C43(DE3) cells. SDS-PAGE (Fig. S3) and Western blot (Fig. 1) analyses of cells sampled during the first 5 h after induction revealed the expression of a protein with an estimated molecular weight (M_w) of ~50 kDa, which agrees with the theoretical M_w of PaPlaB (49.5 kDa). The expression of PaPlaB variants with mutated putative catalytic triad residues S79, D196, and H244 also yielded ~50 kDa proteins as shown by SDS-PAGE (Fig. S4a) and Western blot (Fig. S4b) analyses. Esterase activity assay with the cell lysates revealed that the wild-type PaPlaB was active, but all three variants were inactive (Fig S4c). Hence, their activities were comparable to the activity of the empty vector control.

Considering the membrane localization of the PaPlaB homolog from *L. pneumophila* [19], we suspected the same localization of PaPlaB. This was confirmed by Western blot detection of PaPlaB only in the membrane fraction of *E. coli* C43(DE3) pET22-*paplaB* sedimented upon ultracentrifugation, but no PaPlaB was detected in the soluble fraction containing periplasmic and cytoplasmic proteins (Fig. 1). Furthermore, we incubated membranes containing PaPlaB with buffer containing urea, sodium carbonate, or Triton X-100 to test if PaPlaB is a peripheral or integral membrane protein. Results reveal that PaPlaB was only partially washed from the membrane with

sodium carbonate and urea (Fig. S5). As PaPlaB has no predicted transmembrane helix (Table S5) or β-barrel to permanently attach it to the membrane, it is likely a peripheral membrane-bound protein.

We next investigated whether PaPlaB is associated with the inner or outer membranes of *E. coli* by separating these two membranes using ultracentrifugation in a sucrose density gradient. Analysis of UV absorbance (A_{280nm}) through the gradient after the centrifugation suggested an efficient separation of inner and outer membranes, which we assigned to be fractions 5-7 (inner membranes) and fractions 10-11 (outer membranes) (Fig. 2a). The refractometric measurement showed that the sucrose concentration in fractions 5 and 11 was 45 and 67 % (w/v), respectively, which agrees with the literature [47]. We confirmed that fractions 10-11 contain the outer membrane proteins by immunodetection of the outer membrane protein TolC from *E. coli*, whereas the inner membrane protein SecY was predominantly found in fractions 5-7 (Fig. 2b). Immunodetection of PaPlaB revealed a weak PaPlaB signal in fractions 5-7 and a strong signal in fractions 10-11 (Fig. 2b). However, the highest esterase activity was detected for fraction 5, while the enzymatic activity of the PaPlaB-enriched fraction 11 was negligibly higher than the activity of the empty vector control (Fig. 2c).

For protein isolation, we used Triton X-100 detergent to extract of PaPlaB from the membranes. While mild, non-ionic detergent DDM was added to the buffers used for IMAC purification to maintain the soluble state of PaPlaB. Elution of PaPlaB from Ni^{2+}-NTA column with buffer containing an increasing imidazole concentration resulted in highly pure PaPlaB as judged from SDS-PAGE (Fig. 3). The established protocol yielded ~0.25 mg of PaPlaB per one liter of overexpression culture. Purified PaPlaB showed specific esterase (*p*-NPB substrate) and phospholipase A (1,2-dilauroyl phosphatidylcholine substrate) activities of 3.41 ± 0.1 and 6.74 ± 0.8 *U*/mg, respectively.

As ethylenediaminetetraacetic acid (EDTA), an inhibitor of metal-dependent enzymes, did not exert an inhibitory effect on PaPlaB (Fig. S6), we concluded that PaPlaB belongs to the metal ion-independent type of PLAs [48]. We furthermore examined inhibition of PaPlaB activity with two irreversible inhibitors, paraoxon and phenylmethylsulfonyl fluoride (PMSF) [49]. Under the conditions used, the activity of the paraoxon-treated PaPlaB was abolished (Fig. S6). Paraoxon covalently modifies the catalytic serine residue in the serine-hydrolase enzyme family [50]; therefore, we concluded that PaPlaB contains a nucleophilic serine in its active site, which is in agreement with the sequence-based prediction of a Ser-His-Asp catalytic triad (Fig. S2) and mutational studies (Fig. S4).

3.2 PaPlaB shows promiscuous PLB and lysoPLA activities

Using an esterase activity assay, we observed that PaPlaB retained 100 % of its activity after incubation for 1 h at temperatures up to 42.5^{o}C (Fig. S7). The thermal stability of PaPlaB was confirmed by monitoring its thermal unfolding via changes in the intrinsic fluorescence. The unfolding profile of PaPlaB revealed the transition temperature of ~53°C (Fig. S7). Therefore, a temperature of 37^{o}C, relevant to bacterial infections, was used for *in vitro* activity assays. We next examined the PLA activity of PaPlaB using a spectrum of glycerophospholipids (GPLs) naturally occurring in cell membranes. We showed that PaPlaB is a promiscuous PLA, using GPL substrates with various head groups (ethanolamine, glycerol, and choline) (Fig. 4a) and different fatty acid chain lengths (C6 – C18) (Fig. 4b). It released fatty acids from all tested substrates with specific activities ranging from 2 *U*/mg to 8 *U*/mg, with 1,2-dimyristoyl-phosphatidylethanolamine ($PE_{14:0}$) being the best substrate. We then analyzed whether PaPlaB hydrolyses GPLs containing one fatty acid linked to the *sn*-1 position, called lysoglycerophospholipids (lysoGPLs). Experiments using lysoGPLs with various head groups (ethanolamine, glycerol, and choline) showed that all three lipid types were accepted as substrates by PaPlaB (Fig. 4c). Notably, the lysoPLA activity of PaPlaB is

generally lower (2 – 2.5 *U*/mg) than its PLA activity toward the respective GPLs (Fig. 4c). To analyze whether PaPlaB shows specificity for hydrolysis of fatty acids bound to *sn*-1 or *sn*-2 in GPLs, we tested if PaPlaB hydrolyzes the natural phospholipid 1-oleoyl-2-palmitoyl-PC ($PC_{18:1-16:0}$), which contains different fatty acids bound to glycerol. Spectrophotometric quantification of the total fatty acid amount after incubation of PaPlaB with $PC_{18:1-16:0}$ showed a PaPlaB activity of 3.7 ± 0.6 *U*/mg. To identify which fatty acids were released, PaPlaB-treated $PC_{18:1-16:0}$ samples were analyzed by GC-MS. The results of GC-MS quantification revealed 1.6 ± 0.2 µmol and 1.7 ± 0.1 µmol for palmitic and oleic acid, respectively (Fig. 4d). This result confirmed that PaPlaB hydrolyzes both ester bonds in $PC_{18:1-16:0}$ substrate with a similar efficiency, which classifies it into the phospholipase B (PLB) family.

Next, we tested whether PaPlaB can hydrolyze GPLs reconstituted in SUVs in which GPLs organized in the lipid bilayer resembling the cell membrane. Incubation of PaPlaB with SUVs made of the mixture of DOPE and DOPG resulted in the release of fatty acids from the GPLs (Fig. 4e) while SUVs remained intact as confirmed by DLS analysis (Figs. 4e and S8). Hence, to prevent disruption of SUVs by detergent during the assay, PaPlaB was diluted 10-fold with Tris-HCl (100 mM, pH 8) and detergent was removed by incubation with a nonpolar polystyrene adsorbent. As expected, incubation of SUVs made of DOPG and DOPE with Triton X-100 lead to disruption of SUVs indicated by strong decrease of the average radius determined by DLS (Fig. S8). Conclusively, PaPlaB hydrolyses GPLs from bilayer at a low rate, therefore, no disruption of SUVs was observed.

3.3 PaPlaB oligomerizes in solution

Reversible formation of dimeric and tetrameric LpPlaB was observed at protein concentrations ranging from ~0.01 to 1 mg/ml. Therefore, we assessed whether purified and DDM-stabilized PaPlaB oligomerizes in solution. Size-exclusion chromatography (SEC) analysis of PaPlaB at 0.1, 0.5, and 1.0 mg/ml revealed the presence of several oligomeric PaPlaB species. Protein species of ~45 kDa, and ~360 kDa, as judged through comparison with standard globular proteins of known molecular

weights, were observed for all tested PaPlaB concentrations (Fig. 5a). According to the theoretical M_w of PaPlaB of 49.5 kDa, we can interpret the small-M_w species as monomeric while the exact oligomerization state of high-M_w species cannot be reliably assessed due to detergent bound to PaPlaB and the likely nonglobular shape.

Notably, at low PaPlaB concentration (0.1 mg/ml), the amount of the estimated monomeric PaPlaB is much larger than the amount of the large-M_w oligomers. By raising the PaPlaB concentration to 0.5 and 1 mg/ml, the equilibrium shifts towards large-M_w oligomers, and small-M_w species are depleted. Detection of several intermediate molecular weight species indicates a stepwise and spontaneous oligomerization of PaPlaB. Determination of absolute M_w of protein:detergent complexes by SEC analysis is prone to errors. Therefore, we determined the absolute M_w of DDM-stabilized PaPlaB using multi-angle light scattering coupled to SEC (MALS-SEC). The absolute M_w that was determined at a concentration of 1 mg/ml revealed a distribution starting at ~380 kDa (likely heptamer), which was continuously decreasing to ~50 kDa (monomer) (Fig. 5b). For the PaPlaB sample with 0.1 mg/ml, a very broad MALS signal in the range expected for proteins with M_w ~50 kDa was observed (Fig. S9). Similar to SEC experiments, MALS-SEC results showed that the equilibrium of PaPlaB oligomers depends on the protein concentration.

3.4 PaPlaB is a major cell-associated PLB of *P. aeruginosa* with hydrolytic activity towards endogenous phospholipids

To study the *in vivo* PLB function of PaPlaB in the homologous host, we constructed a *P. aeruginosa* deletion mutant Δ*plaB,* which is missing the entire *plaB* gene (Fig. S1). The activity assay showed a 60 % reduction of cell-associated PLA activity in *P. aeruginosa* Δ*plaB* compared with *P. aeruginosa* wild-type (Fig. 6a). PLA activity of proteins secreted into the medium was not significantly different between these two strains (Fig. 6a), indicating that PaPlaB is a cell-associated and not secreted PLA of *P. aeruginosa*. PLA activity of PaPlaB demonstrated *in vitro* and the membrane localization of the

enzyme provide a hint that PaPlaB function might be related to the hydrolysis of cell membrane GPLs. To test this, we have isolated phospholipids (PLs) from the *P. aeruginosa* wild-type cells by extraction with an organic solvent. These PL extracts were used at 3.3 mg/ml and 0.46 mg/ml as substrates for *in vitro* PLA assay with purified PaPlaB at 450, 45, 4.5 and 0.45 ng/ml.

Results showed that PaPlaB hydrolyzes endogenous PLs with high efficiency (Fig. 6b). Hence, assays with 3.3 mg/ml endogenous PLs showed comparable activities to those measured with $PC_{12:0}$, which was among the best PaPlaB substrates. PaPlaB activity with endogenous PLs was higher at higher substrate concentrations, as expected for enzyme-catalyzed reactions. We furthermore observed that specific PaPlaB activities immensely increase by diluting the PaPlaB samples. Consequently, 2 and > 1100 *U*/mg activities were respectively measured with 450 and 0.45 ng/ml enzyme and 3.3 mg/ml endogenous PLs. We confirmed dilution triggered activation of PaPlaB in the assays performed with 0.46 mg/ml endogenous PLs or $PC_{12:0}$ (Fig 6b).

To analyze if PaPlaB releases FA *in vivo*, we have quantified the intracellular and extracellular FAs in *P. aeruginosa* wild-type and Δ*plaB* cells from the stationary growth phase. GC-MS analysis of FA extracted from cells and cell-free supernatant revealed eight compounds that could be assigned to the following FAs: $C_{16:0}$, $C_{16:1}$ cis-Δ^7, $C_{16:1}$ cis-Δ^9, $C_{17:0}$ cyc(9,10), $C_{18:0}$, $C_{18:1}$ trans-Δ^{11}, $C_{18:1}$ cis-Δ^{11}, $C_{19:0}$ cyc(9,10) (Fig. S10a). The structures of these FAs, previously identified in *P. aeruginosa* [51], were confirmed by mass spectrometry (Figs. S10b-h), and their quantification was achieved by calibration with respective FA standards. This revealed $C_{18:0}$ being significantly (p = 0.02) accumulated in the supernatant of the wild-type compared to Δ*plaB*, although its concentration was not significantly different within the cells (Fig. 6c). Among the other identified FAs only $C_{17:0}$ cyc(9,10) was significantly affected, showing accumulation in the cells of Δ*plaB* (Fig. 6c).

3.5 PaPlaB affects the amount of produced biofilm and its architecture

To investigate whether PaPlaB affects the formation, maturation, and dispersion of biofilm, we have performed long-time studies (8 – 216 h) of biofilm formation in microtiter plates (MTP) under static conditions (crystal violet assay) and in the chamber with a continuous supply of the nutrients under dynamic conditions (confocal laser scanning microscopic (CLSM) analysis). *P. aeruginosa* Δ*plaB* produces significantly less biofilm under static conditions than the wild-type strain after 8, 24, 48, and 72 h of growth, indicating that PaPlaB plays a role in the initial attachment and maturation [52, 53] of *P. aeruginosa* biofilm (Fig. 7a). Under these conditions, the biofilm amount in *P. aeruginosa* Δ*plaB* and wild-type cultures grown for 6 and 9 days showed no significant difference, indicating that PaPlaB likely does not have a function for biofilm dispersion. Based on these results, we examined the biofilm assembly of 24, 72, and 144 h-old biofilms by using CLSM [54]. Large differences between the *P. aeruginosa* Δ*plaB* and WT were observed (Figs. 7b and S11). After 72 h, the wild-type strain forms larger aggregates in contrast to small-sized aggregates observed for the Δ*plaB* strain. The lower density of 72 h-old biofilms found by CLSM correlates with less biofilm quantified by the crystal violet assay after 72 h of growth. Interestingly, although the crystal violet assay did not reveal significant differences after six days of growth, the CLSM showed differences. Hence, the wild-type nearly homogeneously and densely covered the surface of the flow-cell coverslip after 144 h, whereas the Δ*plaB* strain showed less dense coverage indicating impaired maturation [52, 53].

4. Discussion

Here, we identified *P. aeruginosa* PA01 gene *pa2927,* which encodes a novel PLB (PaPlaB) with a function in biofilm assembly. This enzyme shows moderate global sequence homology (Fig. S2) with a known virulence-related outer membrane PLA (LpPlaB) of *L. pneumophila* [18, 19, 43, 44]. The

sequence-based prediction of PLA and lyso-PLA activities of PaPlaB was experimentally confirmed (Fig. 4). Although PaPlaB and LpPlaB have similar biochemical functions, their substrate specificities differ, e.g., PaPlaB shows comparable PLA activities with PG and PC substrates (Fig. 4a), while LpPlaB hydrolyses PG two times faster than PC [18, 19]. Furthermore, a sequence alignment of LpPlaB and PaPlaB revealed strongly conserved catalytic triad residues (Ser79, His244, Asp196 in PaPlaB) (Fig S2) the mutation of which resulted in the loss of PLB activity of these PaPlaB variants (Fig. S4).

We next studied whether PaPlaB is localized within the cell or extracellular protein, as the physiological function of bacterial PLAs and PLBs differ substantially with regard to the cell localization [6, 55]. Extracellular PLA/Bs are toxins involved in host cell membrane disruption [56] or modulation of host cell pathways through the release of bioactive compounds [6]. On the other hand, the function of cell-bound PLA/Bs in bacteria is still not clearly established, although we recently discovered a novel cytoplasmic membrane-bound PLA1 PlaF from *P. aeruginosa*, for which its activity in the remodelling of membrane GPLs is suggested as a virulence mechanism [9, 10]. Interestingly, the function of membrane-bound PLAs for the regulation of the fatty acyl chain composition in GPLs through a deacylation-reacylation pathway called Lands' cycle was described in yeast [57] and other eukaryotes [58].

Using *P. aeruginosa* Δ*plaB*, we observed a ~60 % reduction of a cell-associated PLA activity compared to the wild type, whereas extracellular PLA activities did not significantly differ (Fig. 6a). These results suggest that PaPlaB is the main cell-bound PLA of *P. aeruginosa*. The observed membrane-bound localization of catalytically active PaPlaB recombinantly produced in *E. coli* (Fig. 1) is in agreement with this result, although a large portion was accumulated in catalytically inactive aggregates. Furthermore, activity assays and Western blot analysis of sucrose density gradient-fractionated membranes isolated from fragmented *E. coli* cells overexpressing PaPlaB indicated dual membrane localization of PaPlaB (Fig. 2). The absence of a Western blot signal of PaPlaB in the

520 soluble fraction isolated from *E. coli* cells expressing *paplaB* may be explained by a low
521 concentration of PaPlaB in the cytoplasm or periplasm, which is not surprising for a hydrophobic
522 protein. Interestingly, only the cytoplasmic membrane fraction showed PaPlaB activity, whereas the
523 activity of the outer membrane fraction was comparable to the activity of the negative control
524 strain. The function of PaPlaB may differ in different cellular compartments as described for several,
525 so-called, moonlighting enzymes that catalyze different physiologically relevant reactions in
526 different cellular locations [59].
527 The cellular localization of PaPlaB only partially agrees with the suggested outer-membrane
528 localization of LpPlaB, [43] because LpPlaB showed the highest PLA activity in the outer membrane
529 Momp protein-enriched fractions of *L. pneumophila*. However, it also showed substantial activity
530 (~70 % of outer membrane activity) in the fractions containing inner membranes [43]. The drawback
531 of this fractionation method is the difficulty to exactly separate outer from inner membranes, which
532 was repeatedly described [43, 60, 61]. Keeping in mind that LpPlaB and PaPlaB do not have predicted
533 TM helix or β-barrel-like structures, which were recognized in all hitherto known integral membrane
534 proteins [62, 63], it is likely that these hydrophobic proteins are peripherally associated with one or
535 both membranes. In line with this suggestion is our observation that urea and sodium carbonate
536 destabilized the interaction of PaPlaB with the membrane, as it was shown for other peripheral
537 membrane proteins [64]. These findings strengthen our hypothesis that PaPlaB is a peripheral
538 membrane protein. Interestingly, in PaPlaB and LpPlaB, [43] no recognizable signature for their
539 secretion across the membrane was found; therefore, it remains unknown how these proteins are
540 targeted across the inner membrane and to the outer membrane.
541 Additionally, LpPlaB and PaPlaB are similar in that they homooligomerize at high concentrations,
542 which is accompanied by a decrease in their enzyme activity (Fig. 6b) [44]. Using the SEC method,
543 we observed the equilibrium of PaPlaB monomers and several oligomeric species with M_w of up to

~360 kDa at concentrations 0.1, 0.5, and 1.0 mg/ml. Since the shape, which presumably deviates from a sphere, and bound DDM molecules make it difficult to precisely determinate oligomeric state by SEC, we determined an absolute M_w of PaPlaB by the MALS method. MALS analyses confirmed PaPlaB monomers and the formation of various oligomers of up to ~380 kDa (Fig. 5). The observation that PaPlaB:DDM species of M_w between ~45 and ~380 kDa were simultaneously present in the same sample suggests a stepwise oligomerization of PaPlaB in solution.

SEC and MALS results revealed that increasing the PaPlaB concentration enriches higher oligomeric species. This is similar to LpPlaB, for which only homotetramers were identified at a concentration of ≥ 0.3 mg/ml but a mixture of tetramers and dimers at a concentration ≤ 0.05 mg/ml by analytical ultracentrifugation [44]. Furthermore, the oligomerization at higher protein concentrations was accompanied by several hundredfolds decrease in activities of PaPlaB and LpPlaB (Fig. 6b) [44], which was suggested as a mechanism of protecting the host from uncontrolled degradation of the own membranes [44]. The oligomerization of PaPlaB could open up possibilities for binding different ligands and protein partners in different cellular compartments, thereby regulating its function. This has been suggested for *P. aeruginosa* phospholipase A ExoU [65] and human PLA_2 [66], whose activity is regulated through homomeric and heteromeric protein:protein interactions. Furthermore, for several cytoplasmic moonlighting proteins, it was shown that homoligomerization upon association with the membrane is responsible for acquiring the new functions [59].

Although LpPlaB and PaPlaB seem not to be essential for bacterial life, they both affect important virulence properties of their hosts. It was suggested that the regulation of intracellular replication of *L. pneumophila* is a mechanism of LpPlaB-mediated virulence [43], while the regulation of biofilm maturation is suggested as a mechanism of PaPlaB-mediated virulence (Fig. 7). Although the exact molecular mechanism by which LpPlaB and PaPlaB contribute to bacterial virulence is unknown, phospholipid-degrading activities are likely related to their virulence function. We showed that

PaPlaB rapidly hydrolyses PE (Fig. 4b), which is the most abundant bacterial GPL [51], at the same rate as it hydrolyzes GPLs extracted from the membranes of *P. aeruginosa* (Fig. 6b). We showed that the biochemical function of PaPlaB is related to the complete deacylation of GPLs to fatty acids and glycerophosphoalcohol as shown by lysoPLA assay (Fig. 4c) and GC-MS analysis of fatty acid products released from $PC_{18:1\text{-}16:0}$ (Fig. 4d).

In conclusion, the ability of PaPlaB to rapidly degrade endogenous GPLs in detergent micelles and GPLs in the lipid bilayer (Fig. 4e) and the suggested membrane localization of this novel PLB within *P. aeruginosa* cells open up the questions if a) PaPlaB modulates the molecular GPL profile of bacterial membranes similarly as described for PlaF [9, 10] and PLA_2 from rat [67], yeast [57], and other eukaryotes [58] thus distinguishing it from secreted phospholipase toxins that target host membranes and b) the PLB activity of PaPlaB is directly or indirectly responsible for the observed biofilm phenotype of *P. aeruginosa* Δ*plaB*. It was previously shown that adaptive GPL modulation is important for biofilm formation of *P. aeruginosa,* which undergoes drastic changes in membrane GPL composition upon transition from the planktonic to a biofilm lifestyle [51]. Observed differences in the FA profiles of *P. aeruginosa* wild-type and Δ*plaB* (Fig. 6c) indicate that PaPlaB might be involved in releasing of FAs from endogenous GPLs *in vivo*, or that PaPlaB indirectly changes FA concentration by affecting FA metabolism. The exact role of the catalytic activity of PaPlaB for attachment and biofilm formation of *P. aeruginosa* remains to be elucidated. Our results contribute to a still limited understanding of the virulence mechanism of PLA/B from pathogenic bacteria, which may represent a previously not explored family of antibiotic targets.

Acknowledgment

This study was funded by the Deutsche Forschungsgemeinschaft (DFG, German Research Foundation) – project number 267205415 – CRC 1208 (project A01 to LS, A02 to FK, A03 to HG and A10 to AK). HG is grateful for computational support by the "Zentrum für Informations und Medientechnologie" at the Heinrich-Heine-Universität Düsseldorf and the computing time provided by the John von Neumann Institute for Computing (NIC) to HG on the supercomputer JUWELS at Jülich Supercomputing Centre (JSC) (user IDs: HKF7; VSK33; HDD18). We thank Christoph Strunk, Esther Knieps-Grünhagen, Muttalip Caliskan and Julia Berrger (Heinrich Heine University Düsseldorf, IMET) for their help with the generation of the expression plasmid, SEC analysis, providing *P. aeruginosa* GPLs extract and purified PaPlaB, respectively, and Prof. Karl-Erich Jaeger (Heinrich Heine University Düsseldorf, IMET) for valuable discussions.

Figure legends

Fig. 1: PaPlaB is heterologously expressed in *E. coli*. The expression, localization, and activity of PaPlaB was tested at 1, 2, 3, 4, and 5 h after induction. Cell lysates (10 µl, OD_{580nm} = 10) were analyzed by esterase *p*-NPB assay (top) and Western blotting against the His_6-tag (below). Disrupted cells were fractionated by ultracentrifugation into soluble (cytoplasmic and periplasmic proteins) and membrane protein fractions that were analyzed by Western blotting. *E. coli* C43(DE3) carrying empty vector pET22b were grown under the same conditions and were used as the negative control. Molecular weights of standard proteins (St) are indicated on the right-hand side. The esterase activity results are means ± S.D. of three independent experiments, each set in triplicate.

Fig. 2: Membrane localization of PaPlaB. a) Isolated membranes of *E. coli* C43(DE3) pET-*paplaB* strain cultivated in LB medium (25 ml, 5 h, 37ºC) were separated by sucrose density gradient. *E. coli* C43(DE3) pET22b cultivated under the same conditions was used as the empty vector (EV) control. Fractions (1 ml) were collected, and their sucrose concentration was measured refractometrically (filled circles, dashed line). Protein absorption at 280 nm is shown in solid lines. b) Sucrose density gradient fractions of *E. coli* C43(DE3) pET-*paplaB* were analyzed by Western blotting using the anti-His (C-term)-HRP antibody for detection of PaPlaB and primary anti-TolC and anti-SecY antibodies combined with the anti-rabbit immunoglobulin G antibodies for detection of TolC and SecY from *E. coli*, respectively. The dashed line indicates that anti-SecY figure was combined from two parts of the same Western blot. c) Enzymatic activity was measured with *p*-NPB assay by combining 10 µl of fraction and 150 µl of the substrate. The activities are means ± S.D. of two independent experiments with three samples.

Fig. 3: Purification of detergent-isolated PaPlaB. The fractions eluted from the Ni-NTA column (left) and pooled PaPlaB after desalting by PD-10 column (right) were analyzed by SDS-PAGE (12 % v/v). The molecular weights of protein standards (St) are indicated.

Fig. 4: Phospholipolytic activity profile of PaPlaB. a) PaPlaB is a PLA that hydrolases PE, PG, and PC, which contain unsaturated FAs with C16 (16:0), and C12 (12:0) chain length commonly occurring in *P. aeruginosa* membranes. N.D. = not determined. **b)** Substrate specificity of PaPlaB measured with PE containing different FA chain lengths (C6 - C18). **c)** PaPlaB shows hydrolytic activity towards various lysophospholipids (LPE, LPG, and LPC) containing saturated C16:0 acyl chain. PLA and lysoPLA activities were measured by NEFA-assay using 54 ng PaPlaB per reaction. **d)** GC-MS quantification of oleic ($C_{18:1}$) and palmitic ($C_{16:0}$) fatty acid released by PaPlaB from $PC_{18:1\text{-}16:0}$ substrate. The molar ratio of fatty acids released from *sn*-1 and *sn*-2 position was 51:49, at the reaction equilibrium. e) PaPlaB activity with SUVs made of DOPE:DOPG was measured by quantification of FAs released after 4h incubation with PaPlaB at 37 ºC. Mean ± S.D. of SUV radii and amount (light intensity) were determined by DLS (three experiments, 25 measurements each). PaPlaB buffer was used as the negative control. All activities are mean ± S.D. of three independent experiments with three samples.

Fig. 5: Concentration-dependent oligomerization of PaPlaB. a) PaPlaB (1.0, 0.5, and 0.1 mg/ml), and standard proteins (Table S3) dissolved in a buffer containing DDM were separately analyzed using Biosep-SEC-S3000 column. Proteins were detected by measuring absorbance at 280 nm (solid curves). **b)** SEC-MALS analysis using a Superdex 200 Increase column. PaPlaB (1.0 mg/ml) stabilized by DDM was detected by measuring absorbance at 280 nm (solid curve), and the overall M_w (dashed line) was determined with the software ASTRA 7.

Fig. 6: PaPlaB is a cell-associated PLA of *P. aeruginosa* that releases fatty acids from endogenous phospholipids and cells. a) PLA activity of the whole cells and the supernatant of *P. aeruginosa* wild-type and Δ*plaB* cultivated in LB medium overnight at 37ºC. Cells washed with fresh LB medium were disrupted by ultrasonication before measurement. NEFA assay with $PC_{12:0}$ substrate (25 µl) was performed using cell lysates (25 µl) adjusted to OD_{580nm} = 10 or undiluted cell-free supernatant (25 µl). Results are the means ± S.D. of three measurements with three biological replicates. Statistical analysis was performed using the *t*-test, * $p < 0.05$. b) PLA activity of purified PaPlaB was measured by NEFA assay using endogenous PLs isolated from *P. aeruginosa* wild-type cells and synthetic $PC_{12:0}$, which was used as control. Free fatty acids were quantified after 15 min incubation of PaPlaB with the substrate at 37°C. Activities are mean ± S.D. of three measurements with three biological replicates. c) FAs extracted from *P. aeruginosa* wild-type (3 biological replicates) and Δ*plaB* (4 biological replicates) cells and cell-free supernatant were quantified by GC-MS. Results are mean ± S.D., statistical analysis was performed using the *t*-test, * $p < 0.05$.

Fig. 7: PaPlaB affects biofilm formation in *P. aeruginosa*. a) *P. aeruginosa* wild-type and Δ*plaB* were cultivated in 96-well MTP (LB medium, 37°C, without aeration). The cells not attached to the plastic surface were removed, and the biofilm stained with crystal violet was quantified at 550 nm. The results are mean ± S.D. of three independent experiments with five biological replicates, each measured eight times. Statistical analysis was performed using the *t*-test, *** $p < 0.001$. b) Biofilm architecture analyzed by CLSM after 24, 72, and 144 h growth at 37ºC in a flow cell with continuous supply (50 µl/min) of LB medium. Experiments were repeated two times, each with one biological replicate that was analyzed at three different points by imaging a section of 100 x 100 µm. All collected images are shown in Fig. S12.

References

1. Tacconelli, E., et al., *Discovery, research, and development of new antibiotics: the WHO priority list of antibiotic-resistant bacteria and tuberculosis.* Lancet Infect Dis, 2018. **18**(3): p. 318-327.
2. Filiatrault, M.J., et al., *Identification of* Pseudomonas aeruginosa *genes involved in virulence and anaerobic growth.* Infect Immun, 2006. **74**(7): p. 4237-4245.
3. Werth, B.J., J.J. Carreno, and K.R. Reveles, *Shifting trends in the incidence of* Pseudomonas aeruginosa *septicemia in hospitalized adults in the United States from 1996-2010.* Am J Infect Control, 2015. **43**(5): p. 465-468.
4. Winsor, G.L., et al., *Enhanced annotations and features for comparing thousands of* Pseudomonas *genomes in the* Pseudomonas *genome database.* Nucleic Acids Res, 2016. **44**(D1): p. D646-653.
5. Flores-Diaz, M., et al., *Bacterial sphingomyelinases and phospholipases as virulence factors.* Microbiol Mol Biol Rev, 2016. **80**(3): p. 597-628.
6. Istivan, T.S. and P.J. Coloe, *Phospholipase A in Gram-negative bacteria and its role in pathogenesis.* Microbiology, 2006. **152**(Pt 5): p. 1263-1274.
7. Jaeger, K.E. and F. Kovacic, *Determination of lipolytic enzyme activities.* Methods Mol Biol, 2014. **1149**: p. 111-34.
8. Saliba, A.M., et al., *Eicosanoid-mediated proinflammatory activity of* Pseudomonas aeruginosa *ExoU.* Cell Microbiol, 2005. **7**(12): p. 1811-1822.
9. Kovacic, F., et al., *A membrane-bound esterase PA2949 from* Pseudomonas aeruginosa *is expressed and purified from Escherichia coli.* FEBS Open Bio, 2016. **6**(5): p. 484-93.
10. Bleffert, F., et al., Pseudomonas aeruginosa *esterase PA2949, a bacterial homolog of the human membrane esterase ABHD6: expression, purification and crystallization.* Acta Crystallogr F Struct Biol Commun, 2019. **75**(Pt 4): p. 270-277.
11. Wilhelm, S., et al., *The autotransporter esterase EstA of* Pseudomonas aeruginosa *is required for rhamnolipid production, cell motility, and biofilm formation.* J Bacteriol, 2007. **189**(18): p. 6695-6703.
12. Terada, L.S., et al., Pseudomonas aeruginosa *hemolytic phospholipase C suppresses neutrophil respiratory burst activity.* Infect Immun, 1999. **67**(5): p. 2371-6.
13. Wettstadt, S., et al., *Delivery of the* Pseudomonas aeruginosa *phospholipase effectors PldA and PldB in a VgrG- and H2-T6SS-dependent manner.* Front Microbiol, 2019. **10**(1718): p. 1718.
14. Jiang, F., et al., *A* Pseudomonas aeruginosa *type VI secretion phospholipase D effector targets both prokaryotic and eukaryotic cells.* Cell Host Microbe, 2014. **15**(5): p. 600-610.
15. Hollsing, A.E., et al., *Prospective study of serum antibodies to* Pseudomonas aeruginosa *exoproteins in cystic fibrosis.* J Clin Microbiol, 1987. **25**(10): p. 1868-1874.
16. Rahme, L.G., et al., *Common virulence factors for bacterial pathogenicity in plants and animals.* Science, 1995. **268**(5219): p. 1899-1902.
17. Seipel, K. and A. Flieger, Legionella phospholipases *implicated in infection: determination of enzymatic activities.* Methods Mol Biol, 2013. **954**: p. 355-365.
18. Bender, J., et al., *Phospholipase PlaB of* Legionella pneumophila *represents a novel lipase family: protein residues essential for lipolytic activity, substrate specificity, and hemolysis.* J Biol Chem, 2009. **284**(40): p. 27185-27194.
19. Flieger, A., et al., *Cloning and characterization of the gene encoding the major cell-associated phospholipase A of* Legionella pneumophila*, plaB, exhibiting hemolytic activity.* Infect Immun, 2004. **72**(5): p. 2648-2658.
20. Altschul, S.F., et al., *Basic local alignment search tool.* J Mol Biol, 1990. **215**(3): p. 403-410.
21. Hall, T., Ibis Biosciences, http://www.mbio.ncsu.edu/bioedit/bioedit.html, 2007.
22. Holloway, B.W., V. Krishnapillai, and A.F. Morgan, *Chromosomal genetics of* Pseudomonas*.* Microbiol Rev, 1979. **43**(1): p. 73-102.
23. Kovacic, F., et al., *Structural and functional characterisation of TesA - a novel lysophospholipase A from* Pseudomonas aeruginosa*.* PLoS One, 2013. **8**(7): p. e69125.
24. Woodcock, D.M., et al., *Quantitative evaluation of* Escherichia coli *host strains for tolerance to cytosine methylation in plasmid and phage recombinants.* Nucleic Acids Res, 1989. **17**(9): p. 3469-3478.

25. Miroux, B. and J.E. Walker, *Over-production of proteins in* Escherichia coli*: mutant hosts that allow synthesis of some membrane proteins and globular proteins at high levels.* J Mol Biol, 1996. **260**(3): p. 289-298.
26. Bertani, G., *Studies on lysogenesis. I. The mode of phage liberation by lysogenic* Escherichia coli*.* J Bacteriol, 1951. **62**(3): p. 293-300.
27. Porath, J., et al., *Metal chelate affinity chromatography, a new approach to protein fractionation.* Nature, 1975. **258**: p. 598.
28. Laemmli, U.K., *Cleavage of structural proteins during the assembly of the head of bacteriophage T4.* Nature, 1970. **227**(5259): p. 680-685.
29. Dunn, S.D., *Effects of the modification of transfer buffer composition and the renaturation of proteins in gels on the recognition of proteins on Western blots by monoclonal antibodies.* Anal Biochem, 1986. **157**(1): p. 144-153.
30. Wilkins, M.R., et al., *Protein identification and analysis tools in the ExPASy server.* Methods Mol Biol, 1999. **112**: p. 531-552.
31. Aberle, D., K.-M. Oetter, and G. Meyers, *Lipid binding of the amphipathic helix serving as membrane anchor of pestivirus glycoprotein erns.* PLOS ONE, 2015. **10**(8): p. e0135680.
32. Funada, Y. and Y. Hirata, *Development of a simulation program for the analysis of oils and fats by subcritical fluid chromatography.* Anal Chim Acta, 1999. **401**(1-2): p. 73-82.
33. Yang, Y., et al., *Detection and identification of extra virgin olive oil adulteration by GC-MS combined with chemometrics.* J Agric Food Chem, 2013. **61**(15): p. 3693-3702.
34. Benamara, H., et al., *Characterization of membrane lipidome changes in* Pseudomonas aeruginosa *during biofilm growth on glass wool.* Plos One, 2014. **9**(9): p. e108478.
35. Chao, J., G.M. Wolfaardt, and M.T. Arts, *Characterization of* Pseudomonas aeruginosa *fatty acid profiles in biofilms and batch planktonic cultures.* Can J Microbiol, 2010. **56**(12): p. 1028-1039.
36. Viegas, A., et al., *Structural and dynamic insights revealing how lipase binding domain MD1 of* Pseudomonas aeruginosa *foldase affects lipase activation.* Sci Rep, 2020. **10**(1): p. 3578.
37. Kovacic, F., et al., *Structural features determining thermal adaptation of esterases.* Protein Eng Des Sel, 2016. **29**(2): p. 65-76.
38. Slotboom, D.J., et al., *Static light scattering to characterize membrane proteins in detergent solution.* Methods (San Diego, Calif.), 2008. **46**(2): p. 73-82.
39. Tolker-Nielsen, T. and C. Sternberg, *Growing and analyzing biofilms in flow chambers.* Curr Protoc Microbiol, 2011. **Chapter 1**: p. Unit 1B.2.
40. Martinez-Garcia, E. and V. de Lorenzo, *Engineering multiple genomic deletions in Gram-negative bacteria: Analysis of the multi-resistant antibiotic profile of* Pseudomonas putida *KT2440.* Environ Microbiol, 2011. **13**(10): p. 2702-2716.
41. Coffey, B. and G. Anderson, *Biofilm formation in the 96-well microtiter plate*, in *Pseudomonas Methods and Protocols*, A. Filloux and J.-L. Ramos, Editors. 2014, Springer New York. p. 631-641.
42. Banerji, S., P. Aurass, and A. Flieger, *The manifold phospholipases A of* Legionella pneumophila *- identification, export, regulation, and their link to bacterial virulence.* Int J Med Microbiol, 2008. **298**(3-4): p. 169-181.
43. Schunder, E., et al., *Phospholipase PlaB is a new virulence factor of* Legionella pneumophila*.* Int J Med Microbiol, 2010. **300**(5): p. 313-323.
44. Kuhle, K., et al., *Oligomerization inhibits* Legionella pneumophila *PlaB phospholipase A activity.* J Biol Chem, 2014. **289**(27): p. 18657-18666.
45. Lang, C. and A. Flieger, *Characterisation of* Legionella pneumophila *phospholipases and their impact on host cells.* Eur J Cell Biol, 2011. **90**(11): p. 903-912.
46. Diwo, M., et al., *NAD(H)-mediated tetramerization controls the activity of* Legionella pneumophila *phospholipase PlaB.* PNAS, 2021. **118**(23).
47. Viarre, V., et al., *HxcQ liposecretin is self-piloted to the outer membrane by its N-terminal lipid anchor.* J Biol Chem, 2009. **284**(49): p. 33815-33823.
48. Ramanadham, S., et al., *Calcium-independent phospholipases A2 and their roles in biological processes and diseases.* 2015. **56**(9): p. 1643-1668.

49. Nam, K.H., et al., *The crystal structure of an HSL-homolog EstE5 complex with PMSF reveals a unique configuration that inhibits the nucleophile Ser144 in catalytic triads.* Biochem Biophys Res Commun, 2009. **389**(2): p. 247-50.
50. Asler, I.L., et al., *Mass spectrometric evidence of covalently-bound tetrahydrolipstatin at the catalytic serine of Streptomyces rimosus lipase.* Biochim Biophys Acta, 2007. **1770**(2): p. 163-70.
51. Benamara, H., et al., *Characterization of membrane lipidome changes in Pseudomonas aeruginosa during biofilm growth on glass wool.* PLoS One, 2014. **9**(9): p. e108478.
52. Sauer, K., et al., Pseudomonas aeruginosa *displays multiple phenotypes during development as a biofilm.* J Bacteriol, 2002. **184**(4): p. 1140.
53. Petrova, O.E. and K. Sauer, *A novel signaling network essential for regulating* Pseudomonas aeruginosa *biofilm development.* PLoS pathogens, 2009. **5**(11): p. e1000668.
54. Reichhardt, C. and M.R. Parsek, *Confocal laser scanning microscopy for analysis of* Pseudomonas aeruginosa *biofilm architecture and matrix localization.* Front Microbiol, 2019. **10**: p. 677.
55. Russell, A.B., et al., *Diverse type VI secretion phospholipases are functionally plastic antibacterial effectors.* Nature, 2013. **496**(7446): p. 508-512.
56. Schmiel, D.H. and V.L. Miller, *Bacterial phospholipases and pathogenesis.* Microbes Infect, 1999. **1**(13): p. 1103-1112.
57. Patton-Vogt, J. and A.I.P.M. de Kroon, *Phospholipid turnover and acyl chain remodeling in the yeast ER.* BBA - Mol Cell Biol Lipids, 2020. **1865**(1): p. 158462.
58. Wang, L., et al., *Metabolic interactions between the Lands cycle and the Kennedy pathway of glycerolipid synthesis in* Arabidopsis *developing seeds.* Plant Cell, 2012. **24**(11): p. 4652-4669.
59. Amblee, V. and C.J. Jeffery, *Physical features of intracellular proteins that moonlight on the cell surface.* PLOS ONE, 2015. **10**(6): p. e0130575.
60. Vincent, C.D., et al., *Identification of the core transmembrane complex of the* Legionella *Dot/Icm type IV secretion system.* Mol Microbiol, 2006. **62**(5): p. 1278-91.
61. Eriksson, H.M., et al., *Massive formation of intracellular membrane vesicles in* Escherichia coli *by a monotopic membrane-bound lipid glycosyltransferase.* J Biol Chem, 2009. **284**(49): p. 33904-33914.
62. Craney, A., et al., *Bacterial transmembrane proteins that lack N-terminal signal sequences.* PloS one, 2011. **6**(5): p. e19421.
63. Koebnik, R., K.P. Locher, and P. Van Gelder, *Structure and function of bacterial outer membrane proteins: barrels in a nutshell.* Mol Microbiol, 2000. **37**(2): p. 239-253.
64. Okamoto, T., et al., *Analysis of the association of proteins with membranes.* Curr Protoc Cell Biol, 2001. **Chapter 5**: p. Unit 5.4.
65. Zhang, A., J.L. Veesenmeyer, and A.R. Hauser, *Phosphatidylinositol 4,5-bisphosphate-dependent oligomerization of the* Pseudomonas aeruginosa *cytotoxin ExoU.* Infect Immun, 2017. **86**(1): p. e00402-e00417.
66. Burke, J.E. and E.A. Dennis, *Phospholipase A2 biochemistry.* Cardiovasc Drugs Ther, 2009. **23**(1): p. 49-59.
67. Lands, W.E.M., *Lipid Metabolism.* 1965. **34**(1): p. 313-346.

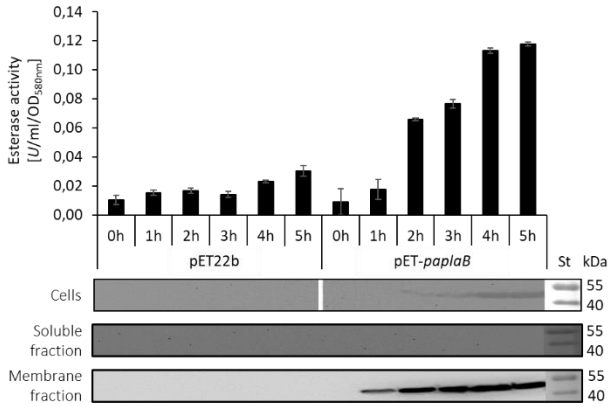

812

813 Figure 1

814

815

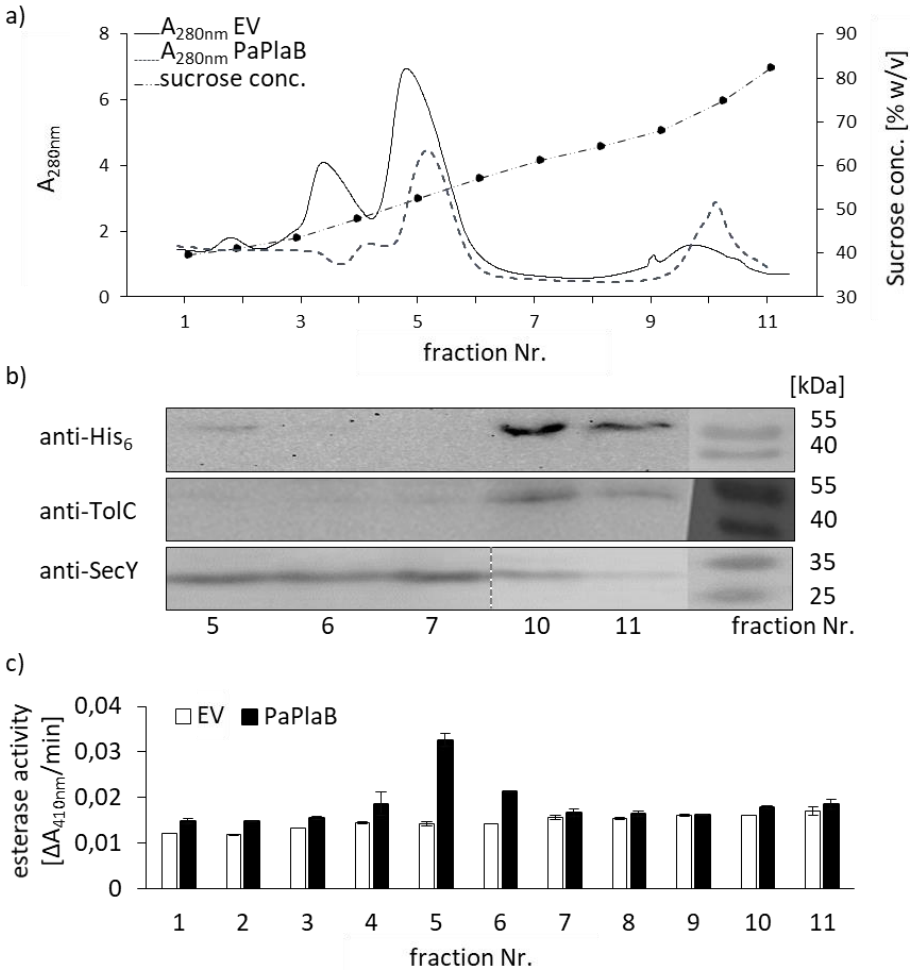

816

817 Figure 2

818

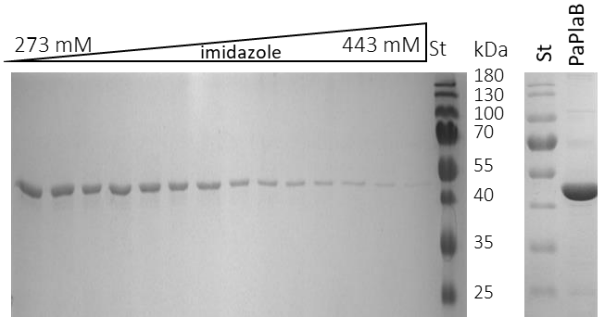
273 mM
imidazole
443 mM
St
kDa
180
130
100
70
55
40
35
25
St
PaPlaB

Figure 3

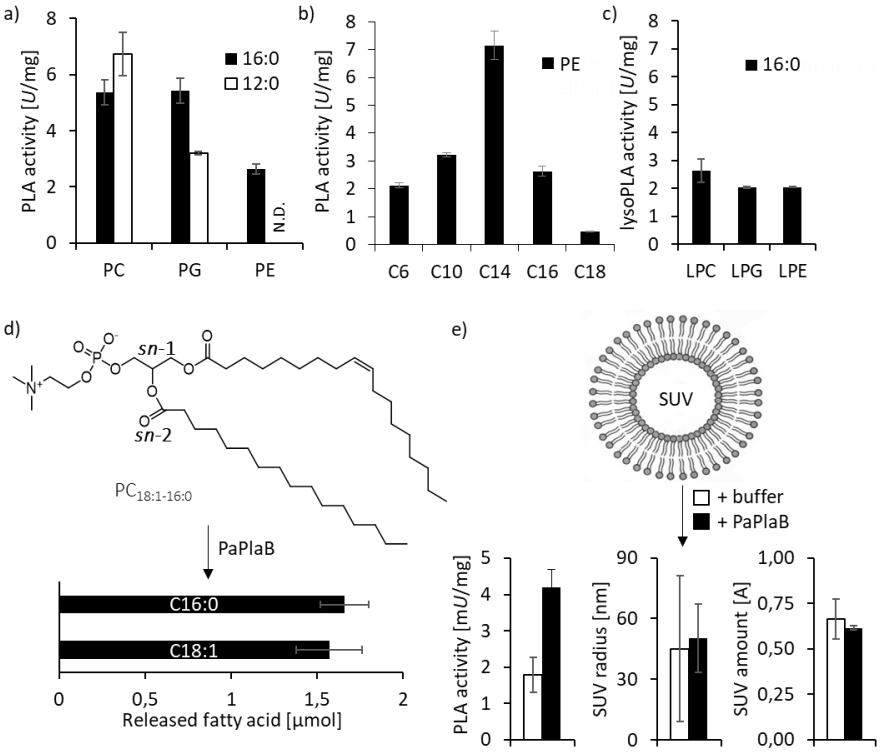

822

823 Figure 4

824

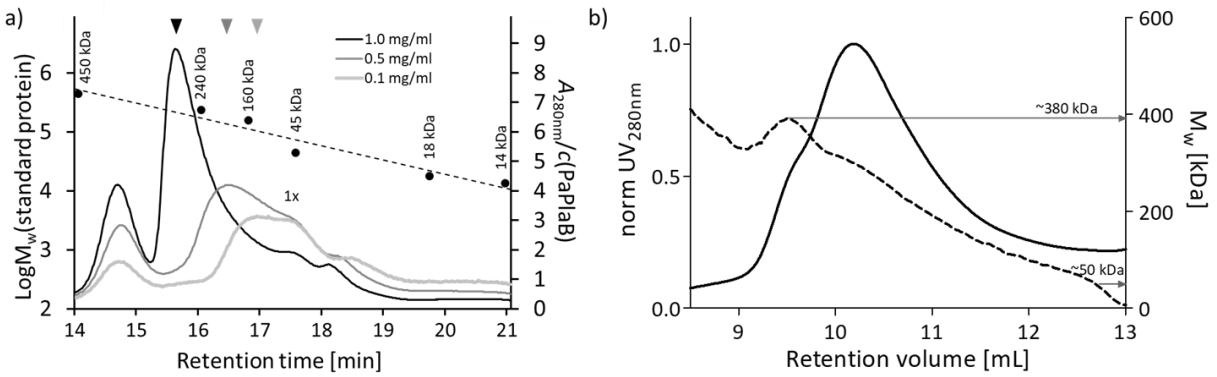

825

826 Figure 5

827

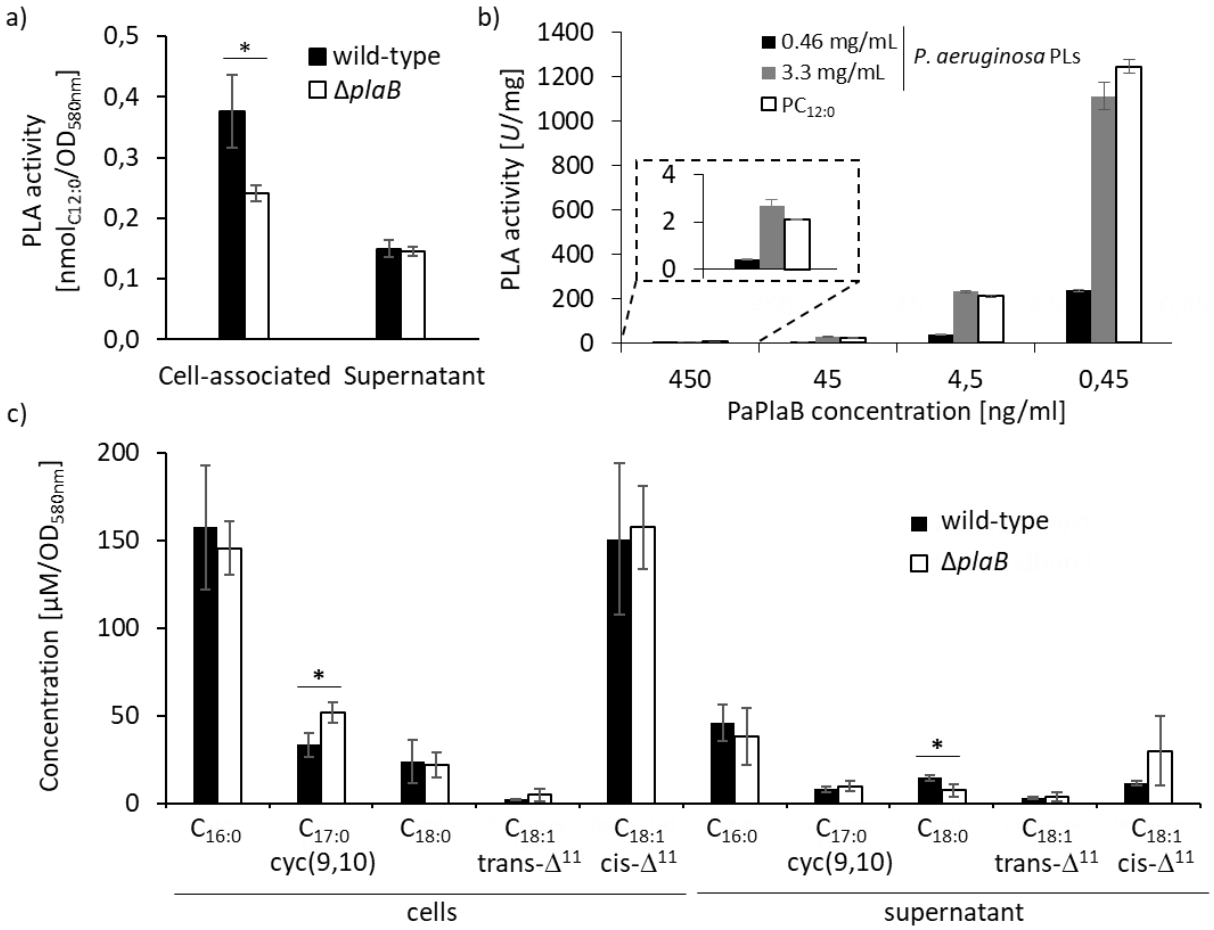
a)
PLA activity [nmol$_{C12:0}$/OD$_{580nm}$]
0,5
0,4
0,3
0,2
0,1
0,0
*
wild-type
Δ*plaB*
Cell-associated
Supernatant
b)
PLA activity [*U*/mg]
1400
1200
1000
800
600
400
200
0
0.46 mg/mL
3.3 mg/mL
PC$_{12:0}$
P. aeruginosa PLs
4
2
0
450
45
4,5
0,45
PaPlaB concentration [ng/ml]
c)
Concentration [µM/OD$_{580nm}$]
200
150
100
50
0
wild-type
Δ*plaB*
*
*
C$_{16:0}$
C$_{17:0}$ cyc(9,10)
C$_{18:0}$
C$_{18:1}$ trans-Δ^{11}
C$_{18:1}$ cis-Δ^{11}
C$_{16:0}$
C$_{17:0}$ cyc(9,10)
C$_{18:0}$
C$_{18:1}$ trans-Δ^{11}
C$_{18:1}$ cis-Δ^{11}
cells
supernatant

Figure 6

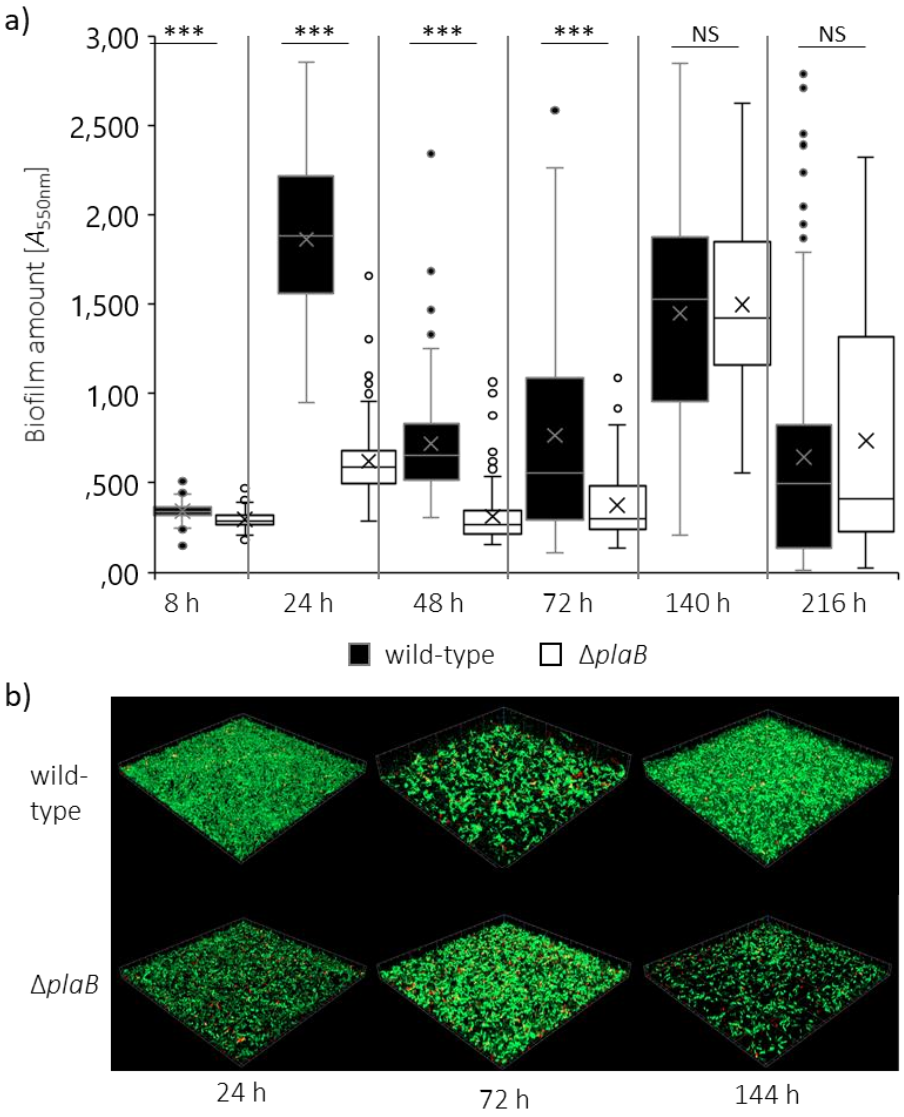
a)
***
***
***
***
NS
NS
3,00
2,500
2,00
1,500
1,00
,500
,00
Biofilm amount [A_{550nm}]
8 h
24 h
48 h
72 h
140 h
216 h
wild-type
ΔplaB
b)
wild-type
ΔplaB
24 h
72 h
144 h

Figure 7

834

A phospholipase B from *Pseudomonas aeruginosa* with activity towards endogenous phospholipids affects biofilm assembly

Andrea J. Weiler[1], Olivia Spitz[2], Mirja Gudzuhn[3], Stephan N. Schott-Verdugo[4,5,7], Michael Kamel[6], Björn Thiele[8], Wolfgang R. Streit[3], Alexej Kedrov[6], Lutz Schmitt[2], Holger Gohlke[4,7] and Filip Kovacic[1,*]

1. Institute of Molecular Enzyme Technology, Heinrich Heine University Düsseldorf, Forschungszentrum Jülich GmbH, D-52425 Jülich, Germany
2. Institute of Biochemistry, Heinrich-Heine-University Düsseldorf, 40225 Düsseldorf, Germany
3. Department of Microbiology and Biotechnology, University of Hamburg, Ohnhorststr. 18, 22609 Hamburg, Germany
4. Institute for Pharmaceutical and Medicinal Chemistry, Heinrich Heine University Düsseldorf, 40225 Düsseldorf, Germany
5. Centro de Bioinformática y Simulación Molecular (CBSM), Facultad de Ingeniería, Universidad de Talca, 2 Norte 685, CL-3460000 Talca, Chile
6. Synthetic Membrane Systems, Institute of Biochemistry, Heinrich Heine University Düsseldorf, 40225 Düsseldorf, Germany
7. John von Neumann Institute for Computing (NIC), Jülich Supercomputing Centre (JSC), Institute of Biological Information Processing (IBI-7: Structural Biochemistry) & Institute of Bio- and Geosciences (IBG-4: Bioinformatics), Forschungszentrum Jülich GmbH, 52425 Jülich, Germany
8. Institute of Bio- and Geosciences, Plant Sciences (IBG-2) and Agrosphere (IBG-3), Forschungszentrum Jülich GmbH, D-52425 Jülich, Germany

* Corresponding author: f.kovacic@fz-juelich.de

Keywords: oligomerization, virulence factor, membrane protein, α/β-hydrolase, pathogen

Abstract

Pseudomonas aeruginosa is a severe threat to immunocompromised patients due to its numerous virulence factors and biofilm-mediated multidrug resistance. It produces and secretes various toxins with hydrolytic activities including phospholipases. However, the function of intracellular phospholipases for bacterial virulence has still not been established. Here, we demonstrate that the hypothetical gene *pa2927* of *P. aeruginosa* encodes a novel phospholipase B named PaPlaB. At reaction equilibrium, PaPlaB purified from detergent-solubilized membranes of *E. coli* released fatty acids (FAs) from *sn*-1 and *sn*-2 positions of phospholipids at the molar ratio of 51:49. PaPlaB *in vitro* hydrolyzed *P. aeruginosa* phospholipids reconstituted in detergent micelles and phospholipids reconstituted in vesicles. Cellular localization studies indicate that PaPlaB is a cell-bound PLA of *P. aeruginosa* and that it is peripherally bound to both membranes in *E. coli*, yet the active form was predominantly associated with the cytoplasmic membrane of *E. coli*. Decreasing the concentration of purified and detergent-stabilized PaPlaB leads to increased enzymatic activity, and at the same time triggers oligomer dissociation. We showed that the free FA profile, biofilm amount and architecture of the wild type and Δ*plaB* differ. However, it remains to be established how the PLB activity of PaPlaB is regulated by homooligomerisation and how it relates to the phenotype of the *P. aeruginosa* Δ*plaB*. This novel putative virulence factor contributes to our understanding of phospholipid degrading enzymes and might provide a target for new therapeutics against *P. aeruginosa* biofilms.

1. Introduction

P. aeruginosa causes severe hospital-associated infections, especially in immunocompromised hosts, which are complicated to treat due to the increasing antibiotic resistance and the aggressive nature of this pathogen leading to the fast progression of the infection [1, 2]. In general, the overall mortality rate determined on a large group of 213,553 patients with *P. aeruginosa* septicemia was 16 %, going along with the observation that the incidence of sepsis has increased since 2001 [3]. This clearly illustrates a need for novel treatments to kill the pathogen or, at least, diminish its virulence. Therefore, the World Health Organization has classified *P. aeruginosa*, together with other "ESKAPE" pathogens including *Enterobacter faecium*, *Staphylococcus aureus*, *Klebsiella pneumoniae*, *Acinetobacter baumannii*, and *Enterobacter spp*., in a priority group for research and development of novel antibiotics. Unfortunately, despite intensive investigations towards understanding the virulence of *P. aeruginosa*, many genes encoding putative virulence factors remain uncharacterized [4].

In *P. aeruginosa*, as well as in other bacterial pathogens, phospholipases, hydrolases with membrane phospholipid-degrading activity, play an important role during infections [5, 6]. They are classified into several groups depending on which ester bond of a glycerophospholipid (GPL) they hydrolyze [7]. While phospholipases C (PLC) and D (PLD), respectively, hydrolyze the glycerol-oriented and the head group-oriented phosphodiester bonds of phospholipids, phospholipases A1 (PLA1) and A2 (PLA2) release fatty acids bound at the *sn*-1 or *sn*-2 positions, respectively. Phospholipases B (PLB) cleave *sn*-1 and *sn*-2 bonds of GPL with similar specificity. Lysophospholipids, degradation products of PLA1 and PLA2, are converted by lysophospholipases A (lysoPLA) to a glycerophosphoalcohol and a fatty acid.

The contribution of bacterial phospholipases to virulence is predominantly related to damaging the host cells, which mostly enhances the survival and spread of the pathogen in the host [5, 6]. Several

phospholipases of *P. aeruginosa*, namely phospholipases A, ExoU [8] and PlaF [9, 10], phospholipase A EstA [11], phospholipase C PlcH [12], and two phospholipases D, PldA and PldB [13], were suggested to be virulence factors in that way. The type III secreted ExoU, and type VI secreted PldA and PldB are directly delivered into eukaryotic cells, where they modulate native host pathways to facilitate invasion by *P. aeruginosa* or inflammation [14]. An EstA of *P. aeruginosa,* which is anchored to the outer membrane with the catalytic domain protruding into the extracellular medium, was shown to affects virulence- and resistance-related phenotypes (cell motility and biofilm formation) [11]. PlcH, one of three secreted PLCs of *P. aeruginosa*, is considered as a virulence factor because (i) it exhibits hemolytic activity; (ii) it is produced during clinical infection with *P. aeruginosa* [15], and (iii) *plcH* deletion strain of *P. aeruginosa* shows attenuated virulence in mouse burn models [16]. However, despite more than three decades of research on phospholipases, still little is known about the direct action of *P. aeruginosa* phospholipases on the bacterial membrane.

On the contrary, one of the best-studied pathogens concerning phospholipases is *Legionella pneumophila,* an intracellularly replicating Gram-negative bacterium [17]. Several phospholipases of *L. pneumophila* were proposed to have a function for establishing a proper life cycle inside a host. One of them is the major surface-associated phospholipase PlaB (LpPlaB). LpPlaB is a serine hydrolase with hemolytic activity and catalytic activity towards common bacterial phospholipids and lysophospholipids containing glycerol and choline head groups [18, 19]. However, the catalytic mechanism of LpPlaB, the mechanism of targeting to the outer membrane, structural features responsible for binding to the membrane, and its effect on the host are unknown.

Here, we expressed, purified, and characterized a homolog of LpPlaB from the human pathogen *P. aeruginosa* PA01, which we named PaPlaB. Comprehensive phospholipolytic enzyme activity studies revealed that PaPlaB is a promiscuous PLB and lysoPLA, which shows strong activity towards endogenous phospholipids isolated from *P. aeruginosa*. Furthermore, we demonstrated that a

P. aeruginosa Δ*plaB* deletion strain produces less biofilm with a different architecture compared to the wild-type bacterium. Thus, the PaPlaB is a novel putative virulence factor of *P. aeruginosa* PA01 belonging to the poorly understood PLB family.

2. Material and methods

2.1 Sequence analysis

Amino acid sequence search and alignment were performed using BLAST and alignment tools provided by the National Center for Biotechnology Information (www.ncbi.nlm.nih.gov) [20]. The sequence alignment was visualized using BioEdit software [21]. TMpred server (https://embnet.vital-it.ch/software/TMPRED_form.html) was used to predict transmembrane helices with the length between 17 and 33 residues. Putative TM helices have TMpred scores above 500.

2.2 Molecular cloning

The *paplaB* gene containing the sequence that encodes a C-terminal His_6-tag was amplified using Phusion® DNA polymerase (Thermo Fisher Scientific, Darmstadt, Germany). In the PCR, the genomic DNA of *P. aeruginosa* PA01 [22], isolated with the DNeasy blood and tissue kit (QIAGEN, Germany), was used as the template together with primers paplaB_for and paplaB_rev (Table S1). The pET22-*paplaB* vector for T7 RNA polymerase-controlled expression of *paplaB* was constructed by ligation of the *paplaB* gene into the pET22b vector (Novagen, Germany) at *Nde*I and *Sac*I restriction sites, using T4 DNA ligase (Thermo Fisher Scientific). Site-directed mutagenesis of PaPlaB was performed by the Quick® Change PCR method using the pET22-*paplaB* plasmid as a template and complementary mutagenic oligonucleotide pairs (Table S1) [23]. *E. coli* DH5α strain [24] was used for molecular cloning experiments. After electrophoresis, the plasmid DNA and DNA fragments from the agarose gel (1 % w/v) were isolated with innuPREP Plasmid Mini Kit 2.0 and the innuPREP

DOUBLEpure Kit (Analytik Jena, Germany), respectively. Oligonucleotides synthesis and plasmid DNA sequencing was performed by Eurofins Genomics (Germany).

2.3 Protein expression and purification

For the expression of PaPlaB with a C-terminal His_6-tag, *E. coli* C43(DE3) [25] cells were transformed with pET22-*paplaB* plasmid, and the empty pET22b vector was used as a control. Cells were grown overnight in lysogeny broth (LB) medium [26] supplemented with ampicillin (100 µg/ml) at 37°C with agitation. Overnight cultures were used to inoculate the expression cultures to an initial OD_{580nm} = 0.05 in LB medium containing ampicillin (100 µg/ml). The cultures were grown at 37°C, and the expression of *paplaB* was induced with isopropyl-β-D-thiogalactoside (IPTG, 1 mM) at OD_{580nm} = 0.4 - 0.6 followed by incubation at 37°C for 5 hours. The cells were harvested by centrifugation (6,000 *g*, 4°C, 10 min) and stored at -20° C before further analysis. Active site variants of PaPlaB carrying S79A, D196A, or H244A mutations were expressed the same way as PaPlaB.

Cells producing PaPlaB were suspended in 100 mM Tris-HCl pH 8, disrupted by a French press, and incubated for 30 min with lysozyme (2 mg/ml) and DNase (0.5 mg/ml). The cell debris and inclusion bodies were removed by centrifugation (6,000 *g*, 4°C, 10 min), and the soluble cell lysate was ultracentrifuged (180,000 *g*, 4°C, 2 h) to isolate the membrane fraction. Subsequently, the proteins were extracted from the membranes upon overnight incubation in the solubilization buffer (5 mM Tris-HCl pH 8, 300 mM NaCl; 50 mM KH_2PO_4; 20 mM imidazole, Triton X-100 1 % v/v) at 4°C. Insoluble debris was removed by ultracentrifugation (180,000 *g*, 4°C, 0.5 h), and the supernatant containing PaPlaB was used for purification.

Immobilized metal affinity chromatographic purification of PaPlaB was performed [27] using the ÄKTA Pure instrument (GE Healthcare). The Ni^{2+}-NTA column (4 ml; Macherey-Nagel, Düren) was equilibrated with ten column volumes of the solubilization buffer before loading the sample. The column was washed with five column volumes of the washing buffer (5 mM Tris-HCl pH 8, 300 mM

NaCl, 50 mM KH_2PO_4, 50 mM imidazole, 0.22 mM DDM) to remove unspecifically bound proteins followed by the elution of PaPlaB with 100 ml of buffer (5 mM Tris-HCl pH 8, 300 mM NaCl, 50 mM KH_2PO_4, 0.22 mM DDM) in which the concentration of imidazole was increased linearly from 50 to 500 mM. The fractions containing pure PaPlaB were transferred into 100 mM Tris-HCl, pH 8 supplemented with 0.22 mM DDM by gel filtration using the PD-10 column (GE Healthcare). Samples were concentrated using an Amicon®Ultra-4 ultrafiltration device, with a cut-off of 10 kDa (Merck Millipore). The protein was incubated at 4°C for 1 h with Bio-Beads™ SM-2 resin (Bio-Rad) equilibrated with 100 mM Tris-HCl, pH 8 to remove excess detergent.

2.4 *In vitro* separation of inner and outer membranes

The separation of the inner and outer membranes of *E. coli* C43(DE3) pET22-*paplaB* (25 ml LB medium, 37°C, 5 h after induction) was performed with a continuous sucrose gradient (20 - 70 % w/v in 100 mM Tris-HCl pH 7.4). The gradients were prepared in SW40-type tubes (Beckman Coulter) using the Gradient Station (Biocomp Instruments, Canada). Isolated membranes were suspended in buffer containing 20 % (w/v) sucrose and loaded on the top of the continuous sucrose gradient followed by ultracentrifugation at 110,000 *g* for 16 h, 4°C in swinging-bucket rotor SW40 (Beckman Coulter). Fractions (1 ml) were collected from the top using the Gradient Station equipped with a TRIAX UV-Vis flow-cell spectrophotometer (Biocomp Instruments, Canada). The sucrose concentration in collected fractions was determined with a refractometer (OPTEC, Optimal Technology, Baldock UK).

2.5 Separation of integral and peripheral bound protein

To identify whether PaPlaB is an integrally or peripherally bound protein, membranes were isolated from *E. coli* C43(DE3) pET22b-*paplaB* expression culture (100 ml). The isolated membranes were suspended in 500 µl of the following buffers: MES buffer as negative control (20 mM, pH 6.5), an aqueous solution of Na_2CO_3 (10 mM), urea (4 M) in MES buffer (20 mM, pH 6.5), Triton X-100 (2%

v/w) in MES buffer (20 mM, pH 6.5). Membranes were incubated at 22 °C for one hour followed by ultracentrifugation at 20,000 *g* for 2 h, 4°C in rotor 55.2 Ti (Beckmann Coulter, California, USA).

2.6 SDS-PAGE and immunodetection

The sodium dodecyl sulfate-polyacrylamide gel electrophoresis (SDS-PAGE) was performed according to the method of Laemmli [28], and the gels were stained with Coomassie Brilliant Blue G-250. For immunodetection of PaPlaB, the gel was loaded with 10 µl of the cell, soluble and membrane fractions isolated from the cell suspension with OD_{580nm} = 25. After SDS-PAGE, proteins were transferred from the gel onto a polyvinylidene difluoride membrane [29] and detected with the anti-His (C-terminal)-HRP antibody (Thermo Fisher/Invitrogen) according to the manufacturer's instructions. The concentration of PaPlaB was determined using the UV-VIS spectrophotometer NanoDrop 2000c (Thermo Fisher Scientific). The extinction coefficient ε = 73.005 M^{-1} cm^{-1} was calculated with the ProtParam tool [30].

2.7 Enzyme activity assay and inhibition

Esterase activity of PaPlaB was determined in a 96-well microtiter plate (MTP) at 37°C by combining 10 µl of enzyme sample with 150 µl of the *p*-nitrophenyl butyrate (*p*-NPB) substrate [7]. Hydrolytic activities towards glycerophospholipids (GPLs) and lysoGPLs (Table S2), which were purchased from Avanti Polar lipids (Alabaster, USA), were determined by quantification of released fatty acids using NEFA assay kit (Wako Chemicals, Neuss, Germany) [7]. Lipids were dissolved in NEFA buffer (50 mM Tris, 100 mM NaCl, 1 mM $CaCl_2$, 1 % (v/v) Triton X-100, pH 7.2). Small unilamellar vesicles (SUVs, 3.3 mg/ml) for enzyme assay were prepared using 1,2-dioleoyl-sn-glycero-3-phospho-(1'-rac-glycerol) (DOPG) and 1,2-dioleoyl-sn-glycero-3-phosphoethanolamine (DOPE) at molar ratio 75 : 20 as described previously [31]. The enzymatic reactions were performed by combining 12.5 µl of enzyme sample with 12.5 µl of a lipid substrate (0.67 mM) at 37°C for 15 min. The enzymatic reactions with SUVs made of DOPE:DOPG were performed by combining 100 µl of enzyme sample with 100 µl of

SUV (3.3 mg/ml) at 37°C for 4h. Prior incubation of PaPlaB with SUVs detergent was removed by incubating 500 µl PaPlaB with 20 BioBeads SM-2 (Bio Rad, Munick, Germany) for 30 min at room temperature. The fatty acid amount was calculated from the calibration curve made with 0.5, 1, 2, 3, 4, and 5 nmol oleic acid.

The inhibition of PaPlaB with PMSF, paraoxon (both were dissolved in propane-2-ol), and EDTA (dissolved in 100 mM Tris-HCl pH 8) was tested as described previously [9]. Inhibition of PaPlaB was performed by incubating enzyme aliquots with the inhibitors for 1.5 h at 30°C, followed by a determination of the enzymatic activity using the *p*-NPB substrate.

2.8 Gas chromatography-mass spectrometric (GC-MS) phospholipase B activity assay

FAs were extracted after 1 h incubation (37°C) of purified PaPlaB (2 ml, 4.28 µg/ml) with 1-oleoyl-2-palmitoyl-PC ($PC_{18:1\text{-}16:0}$; 0.5 mM) in 2 ml NEFA buffer. After incubation, 1 ml of NEFA buffer was added, and FAs were extracted with 12 ml $CHCl_3$: CH_3OH = 2 : 1. The upper chloroform phase was withdrawn, and FAs were extracted again with 8 ml $CHCl_3$. $CHCl_3$ extracts were combined, and $CHCl_3$ was evaporated. FAs were extracted from cells suspended in 20 ml H_2O the same way as described for FA extraction from the supernatant.

FAs were dissolved in 200 µl $CHCl_3$. The $CHCl_3$ extract was mixed with ten volumes of acetonitrile and filtered through a 0.2 µm pore size filter. The residues of the PaPlaB extracts were dissolved in 1 ml acetonitrile : methylenchloride = 4 : 1. Before GC-MS analysis, FAs acids in the PaPlaB extracts and standard solutions were derivatized to trimethylsilylesters. For this purpose, 100 µl of each sample solution was mixed with 700 µl acetonitrile, 100 µl pyridine and 100 µl N-methyl-N-(trimethylsilyl) trifluoroacetamide and heated to 90°C for 1 h. An acetonitrile solution of FAs mixture containing 1 mM $C_{10:0}$, $C_{12:0}$, $C_{14:0}$-, $C_{16:0}$, $C_{18:0}$ and $C_{18:1}$ (oleic acid) was diluted to 50, 100, 200 and 400 µM and derivatized in the same manner as above. The GC-MS system consisted of an Agilent gas chromatograph 7890A and autosampler G4513A (Agilent, CA, USA) coupled to a TOF mass

spectrometer JMS-T100GCV AccuTOF GCv (Jeol, Tokyo, Japan). Analytes were separated on a Zebron-5-HT Inferno column (30 m x 0.25 mm i.d., 0.25 µm film thickness, Phenomenex, USA). Helium was used as carrier gas at a constant gas flow of 1.0 ml/min. The oven temperature program employed for analysis of silylated fatty acids was as follows: 80°C; 5°C/min to 300°C, held for 1 min. The injector temperature was held at 300°C, and all injections (1 µl) were made in the split mode (1:10). The mass spectrometer was used in the electron impact (EI) mode at an ionizing voltage of 70 V and an ionizing current of 300 µA. Analytes were scanned over the range m/z 50 - 750 with a spectrum recording interval of 0.4 s. The GC interface and ion chamber temperature were both kept at 250°C. After the conversion of the raw data files to the cdf-file format, data processing was performed by the use of the software XCalibur 2.0.7 (ThermoFisher Scientific). Fatty acids from the PaPlaB sample were identified by comparison of their retention times and mass spectra with those of fatty acid standards.

2.9 Gas chromatography-mass spectrometric (GC-MS) analysis of FAs extracted from cells

Cells from *P. aeruginosa* PA01 and Δ*plaB* overnight cultures (37˚C, 25 ml LB medium, agitation) were harvested (10 min, 2790×*g*, room temperature) and the supernatant was filtered through a filter with 0.2 µm pore size to remove residual cells. FAs were extracted from supernatant (20 ml) with $CHCl_3$: CH_3OH = 2 : 1 (60 ml). The upper chloroform phase was withdrawn, and FAs were extracted again with 40 ml $CHCl_3$. Chloroform extracts were combined and chloroform was evaporated. FAs were extracted from cells suspended in 20 ml H_2O as described for supernatant.

FAs were transferred to 15 ml Falcon tubes by dissolving in 500 µL CH_2Cl_2 twice. After evaporation to dryness, the remaining fatty acids were derivatized to methyl esters according to Funada et al. with modifications.[32] Briefly, the residues were dissolved in 1 ml sulfuric acid (1 M) in methanol and incubated in an ultrasonic bath for 30 min. The fatty acid methyl esters (FAMEs) were extracted after the addition of 3.3 ml H_2O and 1.7 ml hexane by vigorous shaking for 1 min. The upper organic

phase was withdrawn and dried over sodium carbonate. An aliquote was directly used for GC-MS analysis. A methanol solution of FAs containing 1 mM of $C_{10:0}$, $C_{12:0}$, $C_{14:0}$, $C_{16:0}$, $C_{18:0}$, $C_{17:0}$ (cyc (9,10)), $C_{18:1}$ (cis-Δ9) and $C_{18:1}$ (trans-Δ11) was diluted to 50, 100, 200 and 400 µM and derivatized the same as described above. The Agilent GC-MS system consisted of a gas chromatograph 7890A and an autosampler G4513A coupled to a quadrupole mass spectrometer MS G3172A (Agilent, CA, USA). Analytes were separated on a SGE^{TM} BPX70 column (30 m x 0.32 mm i.d., 0.25 µm film thickness, Thermo Fisher Scientific, USA). Helium was used as carrier gas at a constant gas flow of 1.5 ml/min. The oven temperature program employed for analysis of FAMEs was as follows: 120°C; 20°C/min to 160°C; 3°C/min to 200°C; 20°C to 220°C, held for 8.7 min. The injector temperature was held at 250°C, and all injections (1 µl) were made in the split mode (1:10). The mass spectrometer was used in the electron impact (EI) mode at an ionizing voltage of 70 eV. Analytes were scanned over the range m/z 50 - 400 with a spectrum recording interval of 4 scans/sec. The GC interface temperature was held at 250°C. The MS source and quadrupole temperatures were kept at 280°C and 150°C, respectively. Data processing was performed by use of the software ChemStation E.02.02.1431 (Agilent, CA, USA). Fatty acids from PlaB samples were identified by comparison of their retention times and mass spectra with those of fatty acid standards and published data. [33-35] Quantification of FAMEs C16:0 (1), C17:0 cyc(9,10) (4), C18:0 (5) and C18:1 trans-Δ^{11} (6) (Fig. 1) were performed by external calibration with the corresponding reference compounds. C18:1 cis-Δ^{11} (7) was quantified by use of the calibration curve of oleic acid (C18:1 cis-Δ^{9}) justified by the almost congruent calibration curves of elaidic acid (C18:1 trans-Δ^{9}) and C18:1 trans-Δ^{11}.

2.10 Thermal stability analysis

Differential scanning fluorimetric analysis of PaPlaB thermal stability was performed using the Prometheus NT.48 nanoDSF instrument (NanoTemper Technologies, Germany) [36]. The Prometheus NT.Plex nanoDSF Grade Standard Capillary Chip containing 10 µl PaPlaB sample per

capillary was heated from 20°C to 90°C at the rate of 0.1°C/min, and the intrinsic fluorescence at wavelengths of 330 nm and 350 nm was measured. The first derivative of the ratio of fluorescence intensities at 350 nm and 330 nm as a function of temperature was used to visualize the denaturing transition and determine the "melting" temperature. Enzyme activity-based thermal stability experiments were performed by measuring the residual esterase activity of a PaPlaB sample incubated 1 h at temperatures from 30°C to 70°C [37]. After the incubation, the enzymatic assay was performed as described above using the *p*-NPB substrate, and the inactivation temperature was determined.

2.11 Multi-angle and dynamic light scattering

Superdex 200 Increase 10/300 GL column (GE Healthcare) was equilibrated overnight at a flow rate of 0.6 ml/min with 100 mM Tris pH 8 containing 0.22 mM DDM. For each multi-angle light scattering (MALS) analysis 200 µl PaPlaB at concentrations of 1, 0.5 and 0.1 mg/ml were loaded to the column at the flow rate of 0.6 ml/min using 1260 binary pump (Agilent Technologies), and the scattered light (miniDAWN TREOS II light scatterer, Wyatt Technologies) and the refractive index (Optilab T-rEX refractometer, Wyatt Technologies) were measured. Data analysis was performed with the software ASTRA 7.1.2.5 (Wyatt Technologies) under the assumption that dn/dc of DDM is 0.1435 ml/g and the extinction coefficient of PaPlaB is 1.450 ml/(mg*cm) [38].

Mean diameters of SUVs were determined using SpectroSize 300 dynamic light scattering (DLS) device (Fa. Xtal Concepts, Hamburg). The measurements (25 times, each 20 s) were performed using a 15 µl sample at 20̊C. The viscosity of water of 1.006 cP was used for calculations.

2.12 Size-exclusion chromatography

Size-exclusion chromatographic (SEC) analysis of PaPlaB in Tris-HCl (100 mM, pH 8, 0.22 mM DDM) buffer was performed using Biosep-SEC-S3000 column (Phenomenex, Aschaffenburg, Germany), LC-10Ai isocratic pump (Shimadzu, Duisburg, Germany), and SPD-M20A photodiode array detector

285 (Shimadzu, Duisburg, Germany). The molecular weight (M_w) of standard proteins dissolved in the
286 same buffer as PaPlaB was determined (Table S3). For the analysis, 100 µl of PaPlaB or protein
287 standard sample was loaded on the column, and separation was achieved at a flow rate of 0.5
288 ml/min and 26^{o}C.

289 **2.13 Fluorescence imaging of biofilm in flow chambers**

290 *P. aeruginosa* PAO1 and Δ*plaB* biofilms were grown on a microscope cover glass (24 mm x 50 mm,
291 thickness 0.17 mm, Carl Roth GmbH & Co. KG, Karlsruhe, Germany), which was fixed with PRESIDENT
292 The Original light body silicon (Coltène/Whaledent AG, Altstätten, Switzerland) on the upper side of
293 the three-channel flow chambers [39]. The flow chambers and tubes (standard tubing, ID 0.8 mm,
294 1/16" and Tygon Standard R-3607, ID 1.02 mm; Cole-Parmer GmbH, Wertheim, Germany) were
295 sterilized by flushing with sterile chlorine dioxide spray (Crystel TITANIUM, Tristel Solutions Ltd.,
296 Snailwell, Cambridgeshire, United Kingdom). Afterward, the flow chambers were filled with 1 % (v/v)
297 sodium hypochlorite, and the tubes were autoclaved. All biofilm experiments were performed at
298 37°C with a ten-fold diluted LB medium. Before inoculation, the flow chamber was flushed with 1:10
299 diluted LB medium for 30 minutes with a flow rate of 100 µl/min using the IPC12 High Precision
300 Multichannel Dispenser (Cole-Parmer GmbH, Wertheim, Germany). For inoculation, an overnight
301 culture of *P. aeruginosa* PAO1 or Δ*plaB* was adjusted to an OD_{580nm} of 0.5 in 1:10 diluted LB medium.
302 The diluted culture (300 µl) was inoculated in each channel. After the interruption of medium supply
303 for 1 h, the flow (50 µl/min) was resumed, and the biofilm structure was analyzed after 24, 72, and
304 144 h grown at 37°C. For visualization, the cells were stained with propidium iodide and SYTO 9 dyes
305 using the LIVE/DEAD™ BacLight™ Bacterial Viability Kit (Thermo Fisher Scientific). Imaging of biofilm
306 was performed using the confocal laser scanning microscope (CLSM) Axio Observer.Z1/7 LSM 800
307 with Airyscan (Carl Zeiss Microscopy GmbH, Germany) with the objective C-Apochromat 63x/1.20W
308 Korr UV VisIR. The microscope settings for the different fluorescent dyes are shown in Table S4. The

CLSM images and three-dimensional reconstructions were analysed with the ZEN software (version 2.3, Carl Zeiss Microscopy GmbH, Germany). Experiments were repeated two times, each with one biological replicate that was analyzed at three different points by imaging a section of 100 x 100 µm.

2.14 Construction of *P. aeruginosa* Δ*plaB* strain

The *P. aeruginosa* Δ*plaB* mutant strain was generated by homologous recombination [40]. In short, *P. aeruginosa* PAO1 cells were conjugated with the pEMG-*ΔplaB* mutagenesis vector containing the 814 bp fragment of the upstream region of *paplaB*, followed by a gentamicin resistance gene and the 584 bp downstream region of *paplaB*. For that, *E. coli* S17-1 λpir transformed with the pEMG-*ΔplaB* plasmid was used as a donor strain. *Pseudomonas* cells with pEMG-*ΔplaB* plasmid integrated on the chromosome were selected on LB-agar plates containing gentamicin (30 µg/ml), kanamycin (300 µg/ml; a kanamycin resistance gene is encoded on pEMG plasmid) and irgasan (25 µg/ml; used for negative selection of *E. coli*). Cells transformed with the plasmid pSW-2 containing the I-*Sce*I restriction endonuclease were cultivated on LB agar plates containing benzoic acid (2mM; for induction of I-SceI expression) and irgasan (25 µg/ml). The deletion of the *paplaB* gene was confirmed by PCR amplification using the genomic DNA of *P. aeruginosa ΔplaB* as the template (Fig. S1).

2.15 Crystal violet biofilm assay

P. aeruginosa wild-type and Δ*plaB* cultures incubated in LB medium overnight at 37°C in Erlenmeyer flasks (agitation at 150 rpm) were used to inoculate 100 µl culture with OD_{580nm} 0.1 in plastic 96-well MTP. Cultures were grown at 37°C without agitation, and the cells attached to the surface of MTP after removing the planktonic cells were stained with 0.1 % (w/v) crystal violet solution for 15 min, solubilized with acetic acid (30 % v/v) and quantified spectrophotometrically [41].

3. Results

3.1 Expression of *paplaB* in *E. coli* yields a membrane-bound phospholipase A

P. aeruginosa gene *pa2927* encodes a 49.5 kDa protein that shows moderate sequence similarity (39 %) to LpPlaB (Fig. S2), a major cell-associated PLA of *L. pneumophila* [18, 19, 42-46]. We named the *P. aeruginosa* homolog PaPlaB and set out to experimentally test its sequence-based predicted PLA function. To achieve this, we constructed the PaPlaB expression vector (pET22-*paplaB*) suitable for heterologous expression in *E. coli* strains containing the T7 RNA polymerase gene. *PaplaB* gene in pET22-*paplaB* plasmid was modified by including a sequence coding for six histidine residues at the 3' end to enable purification of the protein using immobilized metal affinity chromatography (IMAC). The protein expression was conducted in *E. coli* C43(DE3) cells. SDS-PAGE (Fig. S3) and Western blot (Fig. 1) analyses of cells sampled during the first 5 h after induction revealed the expression of a protein with an estimated molecular weight (M_w) of ~50 kDa, which agrees with the theoretical M_w of PaPlaB (49.5 kDa). The expression of PaPlaB variants with mutated putative catalytic triad residues S79, D196, and H244 also yielded ~50 kDa proteins as shown by SDS-PAGE (Fig. S4a) and Western blot (Fig. S4b) analyses. Esterase activity assay with the cell lysates revealed that the wild-type PaPlaB was active, but all three variants were inactive (Fig S4c). Hence, their activities were comparable to the activity of the empty vector control.

Considering the membrane localization of the PaPlaB homolog from *L. pneumophila* [19], we suspected the same localization of PaPlaB. This was confirmed by Western blot detection of PaPlaB only in the membrane fraction of *E. coli* C43(DE3) pET22-*paplaB* sedimented upon ultracentrifugation, but no PaPlaB was detected in the soluble fraction containing periplasmic and cytoplasmic proteins (Fig. 1). Furthermore, we incubated membranes containing PaPlaB with buffer containing urea, sodium carbonate, or Triton X-100 to test if PaPlaB is a peripheral or integral membrane protein. Results reveal that PaPlaB was only partially washed from the membrane with

sodium carbonate and urea (Fig. S5). As PaPlaB has no predicted transmembrane helix (Table S5) or β-barrel to permanently attach it to the membrane, it is likely a peripheral membrane-bound protein.

We next investigated whether PaPlaB is associated with the inner or outer membranes of *E. coli* by separating these two membranes using ultracentrifugation in a sucrose density gradient. Analysis of UV absorbance (A_{280nm}) through the gradient after the centrifugation suggested an efficient separation of inner and outer membranes, which we assigned to be fractions 5-7 (inner membranes) and fractions 10-11 (outer membranes) (Fig. 2a). The refractometric measurement showed that the sucrose concentration in fractions 5 and 11 was 45 and 67 % (w/v), respectively, which agrees with the literature [47]. We confirmed that fractions 10-11 contain the outer membrane proteins by immunodetection of the outer membrane protein TolC from *E. coli*, whereas the inner membrane protein SecY was predominantly found in fractions 5-7 (Fig. 2b). Immunodetection of PaPlaB revealed a weak PaPlaB signal in fractions 5-7 and a strong signal in fractions 10-11 (Fig. 2b). However, the highest esterase activity was detected for fraction 5, while the enzymatic activity of the PaPlaB-enriched fraction 11 was negligibly higher than the activity of the empty vector control (Fig. 2c).

For protein isolation, we used Triton X-100 detergent to extract of PaPlaB from the membranes. While mild, non-ionic detergent DDM was added to the buffers used for IMAC purification to maintain the soluble state of PaPlaB. Elution of PaPlaB from Ni^{2+}-NTA column with buffer containing an increasing imidazole concentration resulted in highly pure PaPlaB as judged from SDS-PAGE (Fig. 3). The established protocol yielded ~0.25 mg of PaPlaB per one liter of overexpression culture. Purified PaPlaB showed specific esterase (*p*-NPB substrate) and phospholipase A (1,2-dilauroyl phosphatidylcholine substrate) activities of 3.41 ± 0.1 and 6.74 ± 0.8 *U*/mg, respectively.

As ethylenediaminetetraacetic acid (EDTA), an inhibitor of metal-dependent enzymes, did not exert an inhibitory effect on PaPlaB (Fig. S6), we concluded that PaPlaB belongs to the metal ion-independent type of PLAs [48]. We furthermore examined inhibition of PaPlaB activity with two irreversible inhibitors, paraoxon and phenylmethylsulfonyl fluoride (PMSF) [49]. Under the conditions used, the activity of the paraoxon-treated PaPlaB was abolished (Fig. S6). Paraoxon covalently modifies the catalytic serine residue in the serine-hydrolase enzyme family [50]; therefore, we concluded that PaPlaB contains a nucleophilic serine in its active site, which is in agreement with the sequence-based prediction of a Ser-His-Asp catalytic triad (Fig. S2) and mutational studies (Fig. S4).

3.2 PaPlaB shows promiscuous PLB and lysoPLA activities

Using an esterase activity assay, we observed that PaPlaB retained 100 % of its activity after incubation for 1 h at temperatures up to 42.5^{o}C (Fig. S7). The thermal stability of PaPlaB was confirmed by monitoring its thermal unfolding via changes in the intrinsic fluorescence. The unfolding profile of PaPlaB revealed the transition temperature of ~53°C (Fig. S7). Therefore, a temperature of 37^{o}C, relevant to bacterial infections, was used for *in vitro* activity assays. We next examined the PLA activity of PaPlaB using a spectrum of glycerophospholipids (GPLs) naturally occurring in cell membranes. We showed that PaPlaB is a promiscuous PLA, using GPL substrates with various head groups (ethanolamine, glycerol, and choline) (Fig. 4a) and different fatty acid chain lengths (C6 – C18) (Fig. 4b). It released fatty acids from all tested substrates with specific activities ranging from 2 *U*/mg to 8 *U*/mg, with 1,2-dimyristoyl-phosphatidylethanolamine ($PE_{14:0}$) being the best substrate. We then analyzed whether PaPlaB hydrolyses GPLs containing one fatty acid linked to the *sn*-1 position, called lysoglycerophospholipids (lysoGPLs). Experiments using lysoGPLs with various head groups (ethanolamine, glycerol, and choline) showed that all three lipid types were accepted as substrates by PaPlaB (Fig. 4c). Notably, the lysoPLA activity of PaPlaB is

generally lower (2 – 2.5 *U*/mg) than its PLA activity toward the respective GPLs (Fig. 4c). To analyze whether PaPlaB shows specificity for hydrolysis of fatty acids bound to *sn*-1 or *sn*-2 in GPLs, we tested if PaPlaB hydrolyzes the natural phospholipid 1-oleoyl-2-palmitoyl-PC ($PC_{18:1-16:0}$), which contains different fatty acids bound to glycerol. Spectrophotometric quantification of the total fatty acid amount after incubation of PaPlaB with $PC_{18:1-16:0}$ showed a PaPlaB activity of 3.7 ± 0.6 *U*/mg. To identify which fatty acids were released, PaPlaB-treated $PC_{18:1-16:0}$ samples were analyzed by GC-MS. The results of GC-MS quantification revealed 1.6 ± 0.2 µmol and 1.7 ± 0.1 µmol for palmitic and oleic acid, respectively (Fig. 4d). This result confirmed that PaPlaB hydrolyzes both ester bonds in $PC_{18:1-16:0}$ substrate with a similar efficiency, which classifies it into the phospholipase B (PLB) family.

Next, we tested whether PaPlaB can hydrolyze GPLs reconstituted in SUVs in which GPLs organized in the lipid bilayer resembling the cell membrane. Incubation of PaPlaB with SUVs made of the mixture of DOPE and DOPG resulted in the release of fatty acids from the GPLs (Fig. 4e) while SUVs remained intact as confirmed by DLS analysis (Figs. 4e and S8). Hence, to prevent disruption of SUVs by detergent during the assay, PaPlaB was diluted 10-fold with Tris-HCl (100 mM, pH 8) and detergent was removed by incubation with a nonpolar polystyrene adsorbent. As expected, incubation of SUVs made of DOPG and DOPE with Triton X-100 lead to disruption of SUVs indicated by strong decrease of the average radius determined by DLS (Fig. S8). Conclusively, PaPlaB hydrolyses GPLs from bilayer at a low rate, therefore, no disruption of SUVs was observed.

3.3 PaPlaB oligomerizes in solution

Reversible formation of dimeric and tetrameric LpPlaB was observed at protein concentrations ranging from ~0.01 to 1 mg/ml. Therefore, we assessed whether purified and DDM-stabilized PaPlaB oligomerizes in solution. Size-exclusion chromatography (SEC) analysis of PaPlaB at 0.1, 0.5, and 1.0 mg/ml revealed the presence of several oligomeric PaPlaB species. Protein species of ~45 kDa, and ~360 kDa, as judged through comparison with standard globular proteins of known molecular

weights, were observed for all tested PaPlaB concentrations (Fig. 5a). According to the theoretical M_w of PaPlaB of 49.5 kDa, we can interpret the small-M_w species as monomeric while the exact oligomerization state of high-M_w species cannot be reliably assessed due to detergent bound to PaPlaB and the likely nonglobular shape.

Notably, at low PaPlaB concentration (0.1 mg/ml), the amount of the estimated monomeric PaPlaB is much larger than the amount of the large-M_w oligomers. By raising the PaPlaB concentration to 0.5 and 1 mg/ml, the equilibrium shifts towards large-M_w oligomers, and small-M_w species are depleted. Detection of several intermediate molecular weight species indicates a stepwise and spontaneous oligomerization of PaPlaB. Determination of absolute M_w of protein:detergent complexes by SEC analysis is prone to errors. Therefore, we determined the absolute M_w of DDM-stabilized PaPlaB using multi-angle light scattering coupled to SEC (MALS-SEC). The absolute M_w that was determined at a concentration of 1 mg/ml revealed a distribution starting at ~380 kDa (likely heptamer), which was continuously decreasing to ~50 kDa (monomer) (Fig. 5b). For the PaPlaB sample with 0.1 mg/ml, a very broad MALS signal in the range expected for proteins with M_w ~50 kDa was observed (Fig. S9). Similar to SEC experiments, MALS-SEC results showed that the equilibrium of PaPlaB oligomers depends on the protein concentration.

3.4 PaPlaB is a major cell-associated PLB of *P. aeruginosa* with hydrolytic activity towards endogenous phospholipids

To study the *in vivo* PLB function of PaPlaB in the homologous host, we constructed a *P. aeruginosa* deletion mutant Δ*plaB,* which is missing the entire *plaB* gene (Fig. S1). The activity assay showed a 60 % reduction of cell-associated PLA activity in *P. aeruginosa* Δ*plaB* compared with *P. aeruginosa* wild-type (Fig. 6a). PLA activity of proteins secreted into the medium was not significantly different between these two strains (Fig. 6a), indicating that PaPlaB is a cell-associated and not secreted PLA of *P. aeruginosa*. PLA activity of PaPlaB demonstrated *in vitro* and the membrane localization of the

enzyme provide a hint that PaPlaB function might be related to the hydrolysis of cell membrane GPLs. To test this, we have isolated phospholipids (PLs) from the *P. aeruginosa* wild-type cells by extraction with an organic solvent. These PL extracts were used at 3.3 mg/ml and 0.46 mg/ml as substrates for *in vitro* PLA assay with purified PaPlaB at 450, 45, 4.5 and 0.45 ng/ml.

Results showed that PaPlaB hydrolyzes endogenous PLs with high efficiency (Fig. 6b). Hence, assays with 3.3 mg/ml endogenous PLs showed comparable activities to those measured with $PC_{12:0}$, which was among the best PaPlaB substrates. PaPlaB activity with endogenous PLs was higher at higher substrate concentrations, as expected for enzyme-catalyzed reactions. We furthermore observed that specific PaPlaB activities immensely increase by diluting the PaPlaB samples. Consequently, 2 and > 1100 *U*/mg activities were respectively measured with 450 and 0.45 ng/ml enzyme and 3.3 mg/ml endogenous PLs. We confirmed dilution triggered activation of PaPlaB in the assays performed with 0.46 mg/ml endogenous PLs or $PC_{12:0}$ (Fig 6b).

To analyze if PaPlaB releases FA *in vivo*, we have quantified the intracellular and extracellular FAs in *P. aeruginosa* wild-type and Δ*plaB* cells from the stationary growth phase. GC-MS analysis of FA extracted from cells and cell-free supernatant revealed eight compounds that could be assigned to the following FAs: $C_{16:0}$, $C_{16:1}$ cis-Δ^7, $C_{16:1}$ cis-Δ^9, $C_{17:0}$ cyc(9,10), $C_{18:0}$, $C_{18:1}$ trans-Δ^{11}, $C_{18:1}$ cis-Δ^{11}, $C_{19:0}$ cyc(9,10) (Fig. S10a). The structures of these FAs, previously identified in *P. aeruginosa* [51], were confirmed by mass spectrometry (Figs. S10b-h), and their quantification was achieved by calibration with respective FA standards. This revealed $C_{18:0}$ being significantly (p = 0.02) accumulated in the supernatant of the wild-type compared to Δ*plaB*, although its concentration was not significantly different within the cells (Fig. 6c). Among the other identified FAs only $C_{17:0}$ cyc(9,10) was significantly affected, showing accumulation in the cells of Δ*plaB* (Fig. 6c).

3.5 PaPlaB affects the amount of produced biofilm and its architecture

To investigate whether PaPlaB affects the formation, maturation, and dispersion of biofilm, we have performed long-time studies (8 – 216 h) of biofilm formation in microtiter plates (MTP) under static conditions (crystal violet assay) and in the chamber with a continuous supply of the nutrients under dynamic conditions (confocal laser scanning microscopic (CLSM) analysis). *P. aeruginosa* Δ*plaB* produces significantly less biofilm under static conditions than the wild-type strain after 8, 24, 48, and 72 h of growth, indicating that PaPlaB plays a role in the initial attachment and maturation [52, 53] of *P. aeruginosa* biofilm (Fig. 7a). Under these conditions, the biofilm amount in *P. aeruginosa* Δ*plaB* and wild-type cultures grown for 6 and 9 days showed no significant difference, indicating that PaPlaB likely does not have a function for biofilm dispersion. Based on these results, we examined the biofilm assembly of 24, 72, and 144 h-old biofilms by using CLSM [54]. Large differences between the *P. aeruginosa* Δ*plaB* and WT were observed (Figs. 7b and S11). After 72 h, the wild-type strain forms larger aggregates in contrast to small-sized aggregates observed for the Δ*plaB* strain. The lower density of 72 h-old biofilms found by CLSM correlates with less biofilm quantified by the crystal violet assay after 72 h of growth. Interestingly, although the crystal violet assay did not reveal significant differences after six days of growth, the CLSM showed differences. Hence, the wild-type nearly homogeneously and densely covered the surface of the flow-cell coverslip after 144 h, whereas the Δ*plaB* strain showed less dense coverage indicating impaired maturation [52, 53].

4. Discussion

Here, we identified *P. aeruginosa* PA01 gene *pa2927,* which encodes a novel PLB (PaPlaB) with a function in biofilm assembly. This enzyme shows moderate global sequence homology (Fig. S2) with a known virulence-related outer membrane PLA (LpPlaB) of *L. pneumophila* [18, 19, 43, 44]. The

sequence-based prediction of PLA and lyso-PLA activities of PaPlaB was experimentally confirmed (Fig. 4). Although PaPlaB and LpPlaB have similar biochemical functions, their substrate specificities differ, e.g., PaPlaB shows comparable PLA activities with PG and PC substrates (Fig. 4a), while LpPlaB hydrolyses PG two times faster than PC [18, 19]. Furthermore, a sequence alignment of LpPlaB and PaPlaB revealed strongly conserved catalytic triad residues (Ser79, His244, Asp196 in PaPlaB) (Fig S2) the mutation of which resulted in the loss of PLB activity of these PaPlaB variants (Fig. S4).

We next studied whether PaPlaB is localized within the cell or extracellular protein, as the physiological function of bacterial PLAs and PLBs differ substantially with regard to the cell localization [6, 55]. Extracellular PLA/Bs are toxins involved in host cell membrane disruption [56] or modulation of host cell pathways through the release of bioactive compounds [6]. On the other hand, the function of cell-bound PLA/Bs in bacteria is still not clearly established, although we recently discovered a novel cytoplasmic membrane-bound PLA1 PlaF from *P. aeruginosa*, for which its activity in the remodelling of membrane GPLs is suggested as a virulence mechanism [9, 10]. Interestingly, the function of membrane-bound PLAs for the regulation of the fatty acyl chain composition in GPLs through a deacylation-reacylation pathway called Lands' cycle was described in yeast [57] and other eukaryotes [58].

Using *P. aeruginosa* Δ*plaB*, we observed a ~60 % reduction of a cell-associated PLA activity compared to the wild type, whereas extracellular PLA activities did not significantly differ (Fig. 6a). These results suggest that PaPlaB is the main cell-bound PLA of *P. aeruginosa*. The observed membrane-bound localization of catalytically active PaPlaB recombinantly produced in *E. coli* (Fig. 1) is in agreement with this result, although a large portion was accumulated in catalytically inactive aggregates. Furthermore, activity assays and Western blot analysis of sucrose density gradient-fractionated membranes isolated from fragmented *E. coli* cells overexpressing PaPlaB indicated dual membrane localization of PaPlaB (Fig. 2). The absence of a Western blot signal of PaPlaB in the

soluble fraction isolated from *E. coli* cells expressing *paplaB* may be explained by a low concentration of PaPlaB in the cytoplasm or periplasm, which is not surprising for a hydrophobic protein. Interestingly, only the cytoplasmic membrane fraction showed PaPlaB activity, whereas the activity of the outer membrane fraction was comparable to the activity of the negative control strain. The function of PaPlaB may differ in different cellular compartments as described for several, so-called, moonlighting enzymes that catalyze different physiologically relevant reactions in different cellular locations [59].

The cellular localization of PaPlaB only partially agrees with the suggested outer-membrane localization of LpPlaB, [43] because LpPlaB showed the highest PLA activity in the outer membrane Momp protein-enriched fractions of *L. pneumophila*. However, it also showed substantial activity (~70 % of outer membrane activity) in the fractions containing inner membranes [43]. The drawback of this fractionation method is the difficulty to exactly separate outer from inner membranes, which was repeatedly described [43, 60, 61]. Keeping in mind that LpPlaB and PaPlaB do not have predicted TM helix or β-barrel-like structures, which were recognized in all hitherto known integral membrane proteins [62, 63], it is likely that these hydrophobic proteins are peripherally associated with one or both membranes. In line with this suggestion is our observation that urea and sodium carbonate destabilized the interaction of PaPlaB with the membrane, as it was shown for other peripheral membrane proteins [64]. These findings strengthen our hypothesis that PaPlaB is a peripheral membrane protein. Interestingly, in PaPlaB and LpPlaB, [43] no recognizable signature for their secretion across the membrane was found; therefore, it remains unknown how these proteins are targeted across the inner membrane and to the outer membrane.

Additionally, LpPlaB and PaPlaB are similar in that they homooligomerize at high concentrations, which is accompanied by a decrease in their enzyme activity (Fig. 6b) [44]. Using the SEC method, we observed the equilibrium of PaPlaB monomers and several oligomeric species with M_w of up to

~360 kDa at concentrations 0.1, 0.5, and 1.0 mg/ml. Since the shape, which presumably deviates from a sphere, and bound DDM molecules make it difficult to precisely determinate oligomeric state by SEC, we determined an absolute M_w of PaPlaB by the MALS method. MALS analyses confirmed PaPlaB monomers and the formation of various oligomers of up to ~380 kDa (Fig. 5). The observation that PaPlaB:DDM species of M_w between ~45 and ~380 kDa were simultaneously present in the same sample suggests a stepwise oligomerization of PaPlaB in solution.

SEC and MALS results revealed that increasing the PaPlaB concentration enriches higher oligomeric species. This is similar to LpPlaB, for which only homotetramers were identified at a concentration of ≥ 0.3 mg/ml but a mixture of tetramers and dimers at a concentration ≤ 0.05 mg/ml by analytical ultracentrifugation [44]. Furthermore, the oligomerization at higher protein concentrations was accompanied by several hundredfolds decrease in activities of PaPlaB and LpPlaB (Fig. 6b) [44], which was suggested as a mechanism of protecting the host from uncontrolled degradation of the own membranes [44]. The oligomerization of PaPlaB could open up possibilities for binding different ligands and protein partners in different cellular compartments, thereby regulating its function. This has been suggested for *P. aeruginosa* phospholipase A ExoU [65] and human PLA_2 [66], whose activity is regulated through homomeric and heteromeric protein:protein interactions. Furthermore, for several cytoplasmic moonlighting proteins, it was shown that homoligomerization upon association with the membrane is responsible for acquiring the new functions [59].

Although LpPlaB and PaPlaB seem not to be essential for bacterial life, they both affect important virulence properties of their hosts. It was suggested that the regulation of intracellular replication of *L. pneumophila* is a mechanism of LpPlaB-mediated virulence [43], while the regulation of biofilm maturation is suggested as a mechanism of PaPlaB-mediated virulence (Fig. 7). Although the exact molecular mechanism by which LpPlaB and PaPlaB contribute to bacterial virulence is unknown, phospholipid-degrading activities are likely related to their virulence function. We showed that

PaPlaB rapidly hydrolyses PE (Fig. 4b), which is the most abundant bacterial GPL [51], at the same rate as it hydrolyzes GPLs extracted from the membranes of *P. aeruginosa* (Fig. 6b). We showed that the biochemical function of PaPlaB is related to the complete deacylation of GPLs to fatty acids and glycerophosphoalcohol as shown by lysoPLA assay (Fig. 4c) and GC-MS analysis of fatty acid products released from $PC_{18:1\text{-}16:0}$ (Fig. 4d).

In conclusion, the ability of PaPlaB to rapidly degrade endogenous GPLs in detergent micelles and GPLs in the lipid bilayer (Fig. 4e) and the suggested membrane localization of this novel PLB within *P. aeruginosa* cells open up the questions if a) PaPlaB modulates the molecular GPL profile of bacterial membranes similarly as described for PlaF [9, 10] and PLA_2 from rat [67], yeast [57], and other eukaryotes [58] thus distinguishing it from secreted phospholipase toxins that target host membranes and b) the PLB activity of PaPlaB is directly or indirectly responsible for the observed biofilm phenotype of *P. aeruginosa* Δ*plaB*. It was previously shown that adaptive GPL modulation is important for biofilm formation of *P. aeruginosa,* which undergoes drastic changes in membrane GPL composition upon transition from the planktonic to a biofilm lifestyle [51]. Observed differences in the FA profiles of *P. aeruginosa* wild-type and Δ*plaB* (Fig. 6c) indicate that PaPlaB might be involved in releasing of FAs from endogenous GPLs *in vivo*, or that PaPlaB indirectly changes FA concentration by affecting FA metabolism. The exact role of the catalytic activity of PaPlaB for attachment and biofilm formation of *P. aeruginosa* remains to be elucidated. Our results contribute to a still limited understanding of the virulence mechanism of PLA/B from pathogenic bacteria, which may represent a previously not explored family of antibiotic targets.

Acknowledgment

This study was funded by the Deutsche Forschungsgemeinschaft (DFG, German Research Foundation) – project number 267205415 – CRC 1208 (project A01 to LS, A02 to FK, A03 to HG and A10 to AK). HG is grateful for computational support by the "Zentrum für Informations und Medientechnologie" at the Heinrich-Heine-Universität Düsseldorf and the computing time provided by the John von Neumann Institute for Computing (NIC) to HG on the supercomputer JUWELS at Jülich Supercomputing Centre (JSC) (user IDs: HKF7; VSK33; HDD18). We thank Christoph Strunk, Esther Knieps-Grünhagen, Muttalip Caliskan and Julia Berrger (Heinrich Heine University Düsseldorf, IMET) for their help with the generation of the expression plasmid, SEC analysis, providing *P. aeruginosa* GPLs extract and purified PaPlaB, respectively, and Prof. Karl-Erich Jaeger (Heinrich Heine University Düsseldorf, IMET) for valuable discussions.

600 **Figure legends**
601
602 **Fig. 1: PaPlaB is heterologously expressed in *E. coli*.** The expression, localization, and activity of
603 PaPlaB was tested at 1, 2, 3, 4, and 5 h after induction. Cell lysates (10 µl, OD_{580nm} = 10) were
604 analyzed by esterase *p*-NPB assay (top) and Western blotting against the His_6-tag (below). Disrupted
605 cells were fractionated by ultracentrifugation into soluble (cytoplasmic and periplasmic proteins)
606 and membrane protein fractions that were analyzed by Western blotting. *E. coli* C43(DE3) carrying
607 empty vector pET22b were grown under the same conditions and were used as the negative control.
608 Molecular weights of standard proteins (St) are indicated on the right-hand side. The esterase
609 activity results are means ± S.D. of three independent experiments, each set in triplicate.

610 **Fig. 2: Membrane localization of PaPlaB.** a) Isolated membranes of *E. coli* C43(DE3) pET-*paplaB*
611 strain cultivated in LB medium (25 ml, 5 h, 37ºC) were separated by sucrose density gradient. *E. coli*
612 C43(DE3) pET22b cultivated under the same conditions was used as the empty vector (EV) control.
613 Fractions (1 ml) were collected, and their sucrose concentration was measured refractometrically
614 (filled circles, dashed line). Protein absorption at 280 nm is shown in solid lines. b) Sucrose density
615 gradient fractions of *E. coli* C43(DE3) pET-*paplaB* were analyzed by Western blotting using the anti-
616 His (C-term)-HRP antibody for detection of PaPlaB and primary anti-TolC and anti-SecY antibodies
617 combined with the anti-rabbit immunoglobulin G antibodies for detection of TolC and SecY from *E.*
618 *coli*, respectively. The dashed line indicates that anti-SecY figure was combined from two parts of
619 the same Western blot. c) Enzymatic activity was measured with *p*-NPB assay by combining 10 µl of
620 fraction and 150 µl of the substrate. The activities are means ± S.D. of two independent experiments
621 with three samples.

Fig. 3: Purification of detergent-isolated PaPlaB. The fractions eluted from the Ni-NTA column (left) and pooled PaPlaB after desalting by PD-10 column (right) were analyzed by SDS-PAGE (12 % v/v). The molecular weights of protein standards (St) are indicated.

Fig. 4: Phospholipolytic activity profile of PaPlaB. a) PaPlaB is a PLA that hydrolases PE, PG, and PC, which contain unsaturated FAs with C16 (16:0), and C12 (12:0) chain length commonly occurring in *P. aeruginosa* membranes. N.D. = not determined. **b)** Substrate specificity of PaPlaB measured with PE containing different FA chain lengths (C6 - C18). **c)** PaPlaB shows hydrolytic activity towards various lysophospholipids (LPE, LPG, and LPC) containing saturated C16:0 acyl chain. PLA and lysoPLA activities were measured by NEFA-assay using 54 ng PaPlaB per reaction. **d)** GC-MS quantification of oleic ($C_{18:1}$) and palmitic ($C_{16:0}$) fatty acid released by PaPlaB from $PC_{18:1\text{-}16:0}$ substrate. The molar ratio of fatty acids released from *sn*-1 and *sn*-2 position was 51:49, at the reaction equilibrium. e) PaPlaB activity with SUVs made of DOPE:DOPG was measured by quantification of FAs released after 4h incubation with PaPlaB at 37 ºC. Mean ± S.D. of SUV radii and amount (light intensity) were determined by DLS (three experiments, 25 measurements each). PaPlaB buffer was used as the negative control. All activities are mean ± S.D. of three independent experiments with three samples.

Fig. 5: Concentration-dependent oligomerization of PaPlaB. a) PaPlaB (1.0, 0.5, and 0.1 mg/ml), and standard proteins (Table S3) dissolved in a buffer containing DDM were separately analyzed using Biosep-SEC-S3000 column. Proteins were detected by measuring absorbance at 280 nm (solid curves). **b)** SEC-MALS analysis using a Superdex 200 Increase column. PaPlaB (1.0 mg/ml) stabilized by DDM was detected by measuring absorbance at 280 nm (solid curve), and the overall M_w (dashed line) was determined with the software ASTRA 7.

Fig. 6: PaPlaB is a cell-associated PLA of *P. aeruginosa* that releases fatty acids from endogenous phospholipids and cells. a) PLA activity of the whole cells and the supernatant of *P. aeruginosa* wild-type and Δ*plaB* cultivated in LB medium overnight at 37ºC. Cells washed with fresh LB medium were disrupted by ultrasonication before measurement. NEFA assay with $PC_{12:0}$ substrate (25 µl) was performed using cell lysates (25 µl) adjusted to OD_{580nm} = 10 or undiluted cell-free supernatant (25 µl). Results are the means ± S.D. of three measurements with three biological replicates. Statistical analysis was performed using the *t*-test, * $p < 0.05$. b) PLA activity of purified PaPlaB was measured by NEFA assay using endogenous PLs isolated from *P. aeruginosa* wild-type cells and synthetic $PC_{12:0}$, which was used as control. Free fatty acids were quantified after 15 min incubation of PaPlaB with the substrate at 37°C. Activities are mean ± S.D. of three measurements with three biological replicates. c) FAs extracted from *P. aeruginosa* wild-type (3 biological replicates) and Δ*plaB* (4 biological replicates) cells and cell-free supernatant were quantified by GC-MS. Results are mean ± S.D., statistical analysis was performed using the *t*-test, * $p < 0.05$.

Fig. 7: PaPlaB affects biofilm formation in *P. aeruginosa*. a) *P. aeruginosa* wild-type and Δ*plaB* were cultivated in 96-well MTP (LB medium, 37°C, without aeration). The cells not attached to the plastic surface were removed, and the biofilm stained with crystal violet was quantified at 550 nm. The results are mean ± S.D. of three independent experiments with five biological replicates, each measured eight times. Statistical analysis was performed using the *t*-test, *** $p < 0.001$. b) Biofilm architecture analyzed by CLSM after 24, 72, and 144 h growth at 37ºC in a flow cell with continuous supply (50 µl/min) of LB medium. Experiments were repeated two times, each with one biological replicate that was analyzed at three different points by imaging a section of 100 x 100 µm. All collected images are shown in Fig. S12.

References

1. Tacconelli, E., et al., *Discovery, research, and development of new antibiotics: the WHO priority list of antibiotic-resistant bacteria and tuberculosis.* Lancet Infect Dis, 2018. **18**(3): p. 318-327.
2. Filiatrault, M.J., et al., *Identification of* Pseudomonas aeruginosa *genes involved in virulence and anaerobic growth.* Infect Immun, 2006. **74**(7): p. 4237-4245.
3. Werth, B.J., J.J. Carreno, and K.R. Reveles, *Shifting trends in the incidence of* Pseudomonas aeruginosa *septicemia in hospitalized adults in the United States from 1996-2010.* Am J Infect Control, 2015. **43**(5): p. 465-468.
4. Winsor, G.L., et al., *Enhanced annotations and features for comparing thousands of* Pseudomonas *genomes in the* Pseudomonas *genome database.* Nucleic Acids Res, 2016. **44**(D1): p. D646-653.
5. Flores-Diaz, M., et al., *Bacterial sphingomyelinases and phospholipases as virulence factors.* Microbiol Mol Biol Rev, 2016. **80**(3): p. 597-628.
6. Istivan, T.S. and P.J. Coloe, *Phospholipase A in Gram-negative bacteria and its role in pathogenesis.* Microbiology, 2006. **152**(Pt 5): p. 1263-1274.
7. Jaeger, K.E. and F. Kovacic, *Determination of lipolytic enzyme activities.* Methods Mol Biol, 2014. **1149**: p. 111-34.
8. Saliba, A.M., et al., *Eicosanoid-mediated proinflammatory activity of* Pseudomonas aeruginosa *ExoU.* Cell Microbiol, 2005. **7**(12): p. 1811-1822.
9. Kovacic, F., et al., *A membrane-bound esterase PA2949 from* Pseudomonas aeruginosa *is expressed and purified from Escherichia coli.* FEBS Open Bio, 2016. **6**(5): p. 484-93.
10. Bleffert, F., et al., Pseudomonas aeruginosa *esterase PA2949, a bacterial homolog of the human membrane esterase ABHD6: expression, purification and crystallization.* Acta Crystallogr F Struct Biol Commun, 2019. **75**(Pt 4): p. 270-277.
11. Wilhelm, S., et al., *The autotransporter esterase EstA of* Pseudomonas aeruginosa *is required for rhamnolipid production, cell motility, and biofilm formation.* J Bacteriol, 2007. **189**(18): p. 6695-6703.
12. Terada, L.S., et al., Pseudomonas aeruginosa *hemolytic phospholipase C suppresses neutrophil respiratory burst activity.* Infect Immun, 1999. **67**(5): p. 2371-6.
13. Wettstadt, S., et al., *Delivery of the* Pseudomonas aeruginosa *phospholipase effectors PldA and PldB in a VgrG- and H2-T6SS-dependent manner.* Front Microbiol, 2019. **10**(1718): p. 1718.
14. Jiang, F., et al., *A* Pseudomonas aeruginosa *type VI secretion phospholipase D effector targets both prokaryotic and eukaryotic cells.* Cell Host Microbe, 2014. **15**(5): p. 600-610.
15. Hollsing, A.E., et al., *Prospective study of serum antibodies to* Pseudomonas aeruginosa *exoproteins in cystic fibrosis.* J Clin Microbiol, 1987. **25**(10): p. 1868-1874.
16. Rahme, L.G., et al., *Common virulence factors for bacterial pathogenicity in plants and animals.* Science, 1995. **268**(5219): p. 1899-1902.
17. Seipel, K. and A. Flieger, Legionella phospholipases *implicated in infection: determination of enzymatic activities.* Methods Mol Biol, 2013. **954**: p. 355-365.
18. Bender, J., et al., *Phospholipase PlaB of* Legionella pneumophila *represents a novel lipase family: protein residues essential for lipolytic activity, substrate specificity, and hemolysis.* J Biol Chem, 2009. **284**(40): p. 27185-27194.
19. Flieger, A., et al., *Cloning and characterization of the gene encoding the major cell-associated phospholipase A of* Legionella pneumophila*, plaB, exhibiting hemolytic activity.* Infect Immun, 2004. **72**(5): p. 2648-2658.
20. Altschul, S.F., et al., *Basic local alignment search tool.* J Mol Biol, 1990. **215**(3): p. 403-410.
21. Hall, T., Ibis Biosciences, http://www.mbio.ncsu.edu/bioedit/bioedit.html, 2007.
22. Holloway, B.W., V. Krishnapillai, and A.F. Morgan, *Chromosomal genetics of* Pseudomonas*.* Microbiol Rev, 1979. **43**(1): p. 73-102.
23. Kovacic, F., et al., *Structural and functional characterisation of TesA - a novel lysophospholipase A from* Pseudomonas aeruginosa*.* PLoS One, 2013. **8**(7): p. e69125.
24. Woodcock, D.M., et al., *Quantitative evaluation of* Escherichia coli *host strains for tolerance to cytosine methylation in plasmid and phage recombinants.* Nucleic Acids Res, 1989. **17**(9): p. 3469-3478.

25. Miroux, B. and J.E. Walker, *Over-production of proteins in* Escherichia coli*: mutant hosts that allow synthesis of some membrane proteins and globular proteins at high levels.* J Mol Biol, 1996. **260**(3): p. 289-298.
26. Bertani, G., *Studies on lysogenesis. I. The mode of phage liberation by lysogenic* Escherichia coli. J Bacteriol, 1951. **62**(3): p. 293-300.
27. Porath, J., et al., *Metal chelate affinity chromatography, a new approach to protein fractionation.* Nature, 1975. **258**: p. 598.
28. Laemmli, U.K., *Cleavage of structural proteins during the assembly of the head of bacteriophage T4.* Nature, 1970. **227**(5259): p. 680-685.
29. Dunn, S.D., *Effects of the modification of transfer buffer composition and the renaturation of proteins in gels on the recognition of proteins on Western blots by monoclonal antibodies.* Anal Biochem, 1986. **157**(1): p. 144-153.
30. Wilkins, M.R., et al., *Protein identification and analysis tools in the ExPASy server.* Methods Mol Biol, 1999. **112**: p. 531-552.
31. Aberle, D., K.-M. Oetter, and G. Meyers, *Lipid binding of the amphipathic helix serving as membrane anchor of pestivirus glycoprotein erns.* PLOS ONE, 2015. **10**(8): p. e0135680.
32. Funada, Y. and Y. Hirata, *Development of a simulation program for the analysis of oils and fats by subcritical fluid chromatography.* Anal Chim Acta, 1999. **401**(1-2): p. 73-82.
33. Yang, Y., et al., *Detection and identification of extra virgin olive oil adulteration by GC-MS combined with chemometrics.* J Agric Food Chem, 2013. **61**(15): p. 3693-3702.
34. Benamara, H., et al., *Characterization of membrane lipidome changes in* Pseudomonas aeruginosa *during biofilm growth on glass wool.* Plos One, 2014. **9**(9): p. e108478.
35. Chao, J., G.M. Wolfaardt, and M.T. Arts, *Characterization of* Pseudomonas aeruginosa *fatty acid profiles in biofilms and batch planktonic cultures.* Can J Microbiol, 2010. **56**(12): p. 1028-1039.
36. Viegas, A., et al., *Structural and dynamic insights revealing how lipase binding domain MD1 of* Pseudomonas aeruginosa *foldase affects lipase activation.* Sci Rep, 2020. **10**(1): p. 3578.
37. Kovacic, F., et al., *Structural features determining thermal adaptation of esterases.* Protein Eng Des Sel, 2016. **29**(2): p. 65-76.
38. Slotboom, D.J., et al., *Static light scattering to characterize membrane proteins in detergent solution.* Methods (San Diego, Calif.), 2008. **46**(2): p. 73-82.
39. Tolker-Nielsen, T. and C. Sternberg, *Growing and analyzing biofilms in flow chambers.* Curr Protoc Microbiol, 2011. **Chapter 1**: p. Unit 1B.2.
40. Martinez-Garcia, E. and V. de Lorenzo, *Engineering multiple genomic deletions in Gram-negative bacteria: Analysis of the multi-resistant antibiotic profile of* Pseudomonas putida *KT2440.* Environ Microbiol, 2011. **13**(10): p. 2702-2716.
41. Coffey, B. and G. Anderson, *Biofilm formation in the 96-well microtiter plate*, in *Pseudomonas Methods and Protocols*, A. Filloux and J.-L. Ramos, Editors. 2014, Springer New York. p. 631-641.
42. Banerji, S., P. Aurass, and A. Flieger, *The manifold phospholipases A of* Legionella pneumophila *- identification, export, regulation, and their link to bacterial virulence.* Int J Med Microbiol, 2008. **298**(3-4): p. 169-181.
43. Schunder, E., et al., *Phospholipase PlaB is a new virulence factor of* Legionella pneumophila*.* Int J Med Microbiol, 2010. **300**(5): p. 313-323.
44. Kuhle, K., et al., *Oligomerization inhibits* Legionella pneumophila *PlaB phospholipase A activity.* J Biol Chem, 2014. **289**(27): p. 18657-18666.
45. Lang, C. and A. Flieger, *Characterisation of* Legionella pneumophila *phospholipases and their impact on host cells.* Eur J Cell Biol, 2011. **90**(11): p. 903-912.
46. Diwo, M., et al., *NAD(H)-mediated tetramerization controls the activity of* Legionella pneumophila *phospholipase PlaB.* PNAS, 2021. **118**(23).
47. Viarre, V., et al., *HxcQ liposecretin is self-piloted to the outer membrane by its N-terminal lipid anchor.* J Biol Chem, 2009. **284**(49): p. 33815-33823.
48. Ramanadham, S., et al., *Calcium-independent phospholipases A2 and their roles in biological processes and diseases.* 2015. **56**(9): p. 1643-1668.

49. Nam, K.H., et al., *The crystal structure of an HSL-homolog EstE5 complex with PMSF reveals a unique configuration that inhibits the nucleophile Ser144 in catalytic triads.* Biochem Biophys Res Commun, 2009. **389**(2): p. 247-50.
50. Asler, I.L., et al., *Mass spectrometric evidence of covalently-bound tetrahydrolipstatin at the catalytic serine of Streptomyces rimosus lipase.* Biochim Biophys Acta, 2007. **1770**(2): p. 163-70.
51. Benamara, H., et al., *Characterization of membrane lipidome changes in Pseudomonas aeruginosa during biofilm growth on glass wool.* PLoS One, 2014. **9**(9): p. e108478.
52. Sauer, K., et al., Pseudomonas aeruginosa *displays multiple phenotypes during development as a biofilm.* J Bacteriol, 2002. **184**(4): p. 1140.
53. Petrova, O.E. and K. Sauer, *A novel signaling network essential for regulating* Pseudomonas aeruginosa *biofilm development.* PLoS pathogens, 2009. **5**(11): p. e1000668.
54. Reichhardt, C. and M.R. Parsek, *Confocal laser scanning microscopy for analysis of* Pseudomonas aeruginosa *biofilm architecture and matrix localization.* Front Microbiol, 2019. **10**: p. 677.
55. Russell, A.B., et al., *Diverse type VI secretion phospholipases are functionally plastic antibacterial effectors.* Nature, 2013. **496**(7446): p. 508-512.
56. Schmiel, D.H. and V.L. Miller, *Bacterial phospholipases and pathogenesis.* Microbes Infect, 1999. **1**(13): p. 1103-1112.
57. Patton-Vogt, J. and A.I.P.M. de Kroon, *Phospholipid turnover and acyl chain remodeling in the yeast ER.* BBA - Mol Cell Biol Lipids, 2020. **1865**(1): p. 158462.
58. Wang, L., et al., *Metabolic interactions between the Lands cycle and the Kennedy pathway of glycerolipid synthesis in* Arabidopsis *developing seeds.* Plant Cell, 2012. **24**(11): p. 4652-4669.
59. Amblee, V. and C.J. Jeffery, *Physical features of intracellular proteins that moonlight on the cell surface.* PLOS ONE, 2015. **10**(6): p. e0130575.
60. Vincent, C.D., et al., *Identification of the core transmembrane complex of the* Legionella *Dot/Icm type IV secretion system.* Mol Microbiol, 2006. **62**(5): p. 1278-91.
61. Eriksson, H.M., et al., *Massive formation of intracellular membrane vesicles in* Escherichia coli *by a monotopic membrane-bound lipid glycosyltransferase.* J Biol Chem, 2009. **284**(49): p. 33904-33914.
62. Craney, A., et al., *Bacterial transmembrane proteins that lack N-terminal signal sequences.* PloS one, 2011. **6**(5): p. e19421.
63. Koebnik, R., K.P. Locher, and P. Van Gelder, *Structure and function of bacterial outer membrane proteins: barrels in a nutshell.* Mol Microbiol, 2000. **37**(2): p. 239-253.
64. Okamoto, T., et al., *Analysis of the association of proteins with membranes.* Curr Protoc Cell Biol, 2001. **Chapter 5**: p. Unit 5.4.
65. Zhang, A., J.L. Veesenmeyer, and A.R. Hauser, *Phosphatidylinositol 4,5-bisphosphate-dependent oligomerization of the* Pseudomonas aeruginosa *cytotoxin ExoU.* Infect Immun, 2017. **86**(1): p. e00402-e00417.
66. Burke, J.E. and E.A. Dennis, *Phospholipase A2 biochemistry.* Cardiovasc Drugs Ther, 2009. **23**(1): p. 49-59.
67. Lands, W.E.M., *Lipid Metabolism.* 1965. **34**(1): p. 313-346.

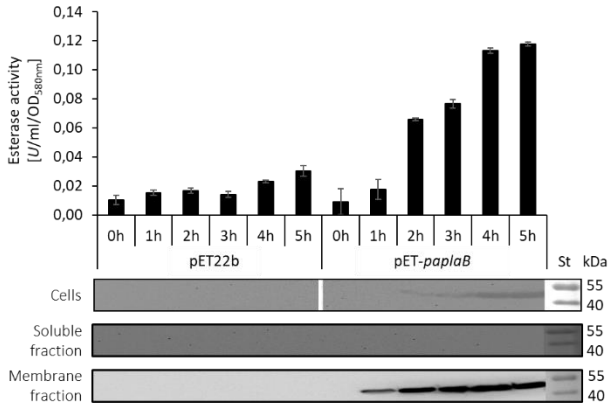

812

813 Figure 1

814

815

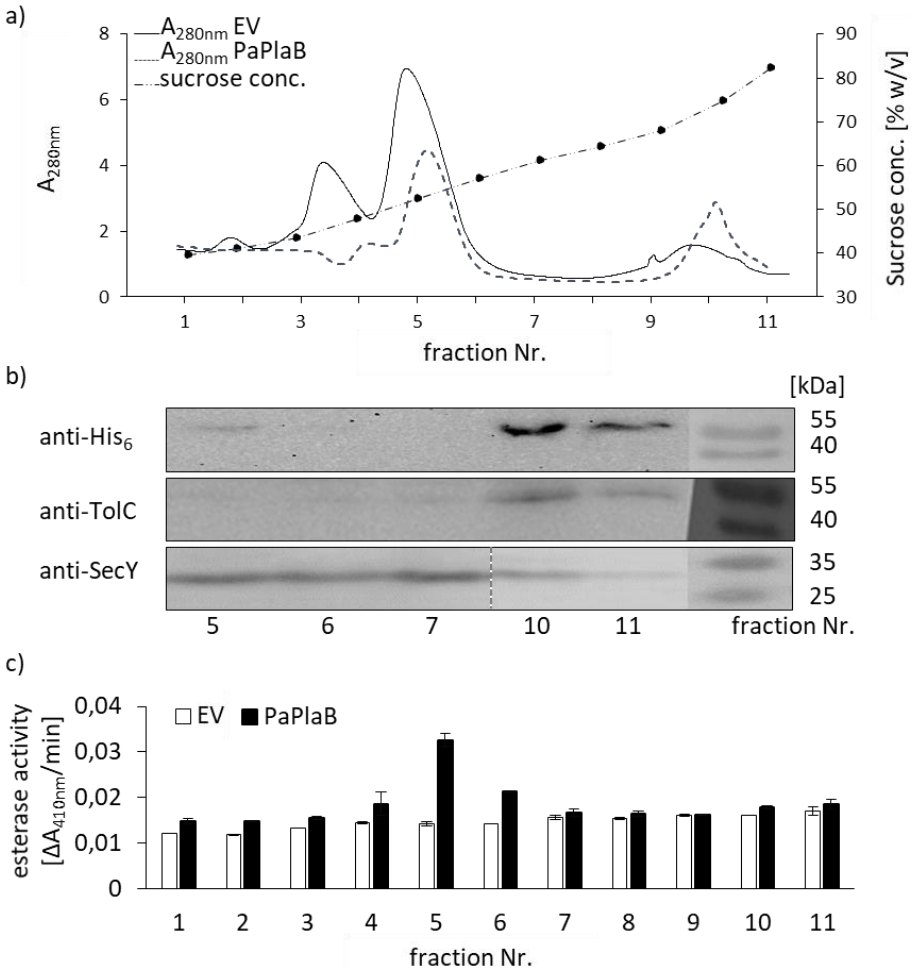

816

817 Figure 2

818

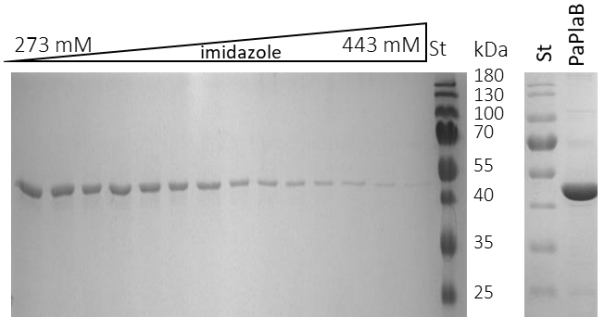
273 mM
imidazole
443 mM
St
kDa
180
130
100
70
55
40
35
25
St
PaPlaB

Figure 3

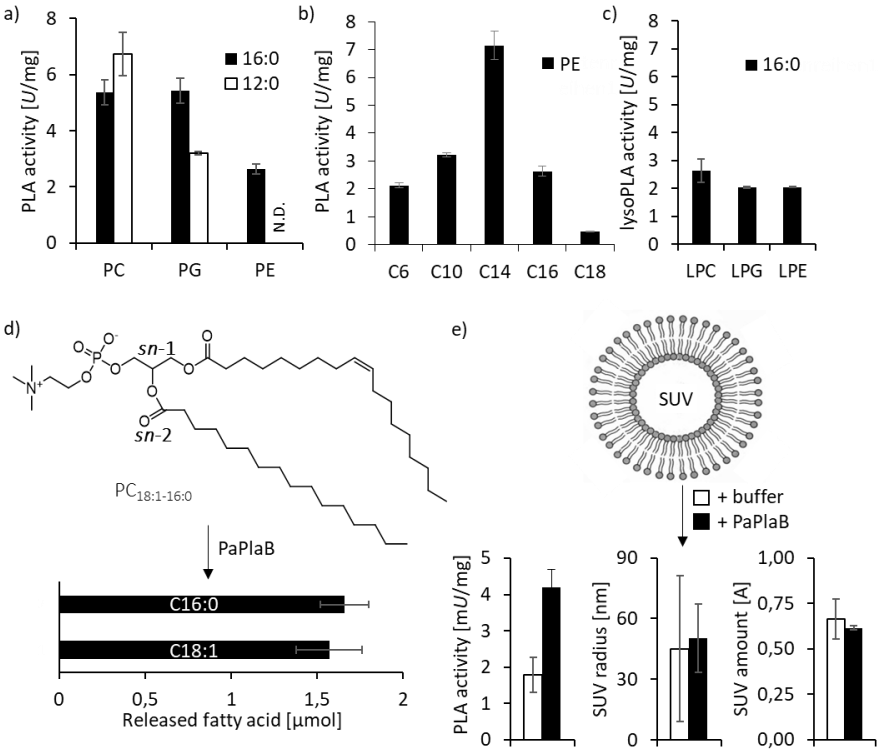

822

823 Figure 4

824

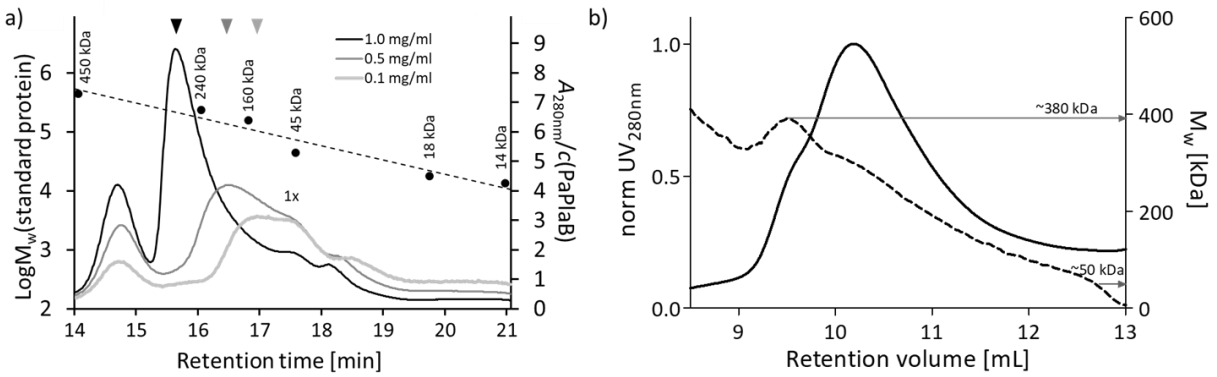

825

826 Figure 5

827

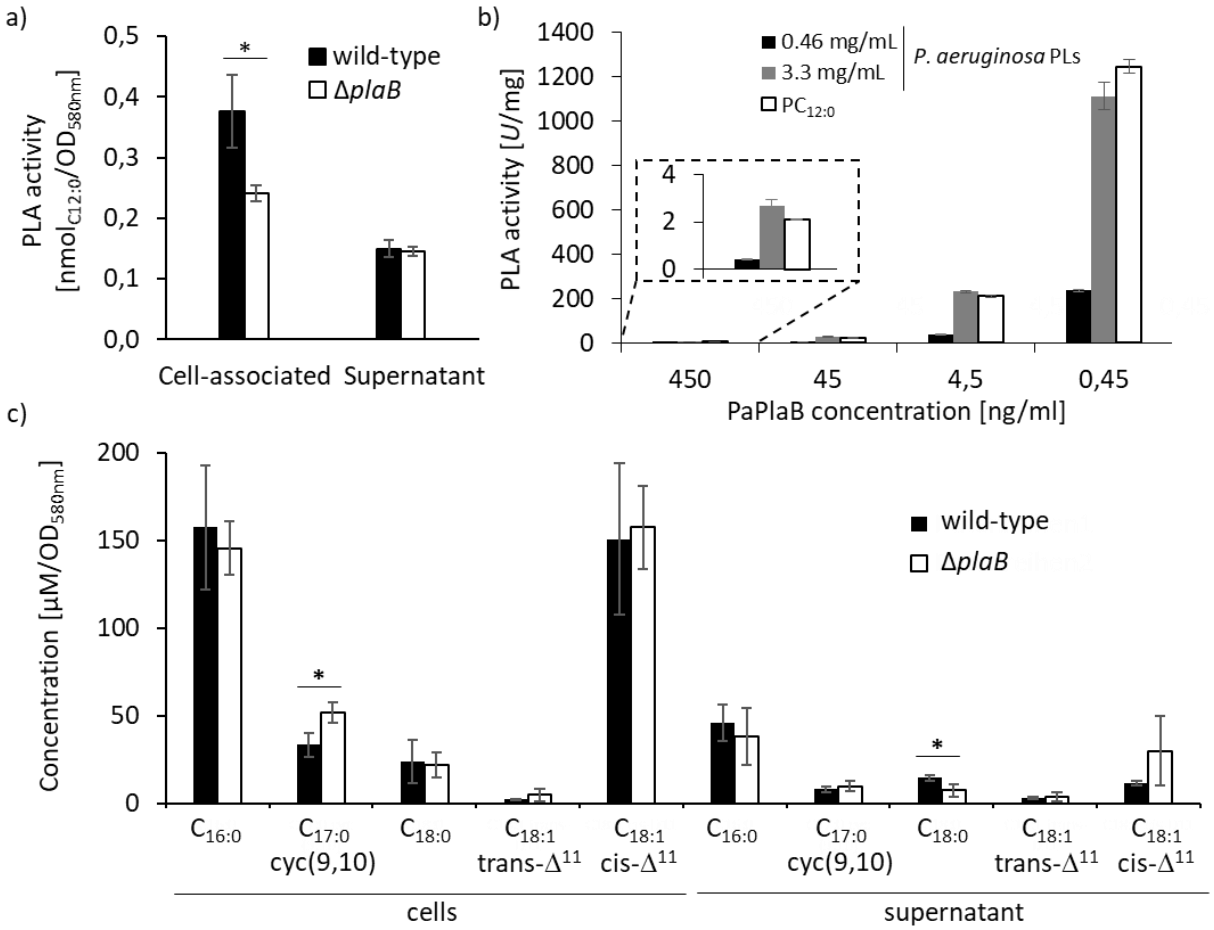
a)
PLA activity [nmol$_{C12:0}$/OD$_{580nm}$]
0,5
0,4
0,3
0,2
0,1
0,0
*
wild-type
Δ*plaB*
Cell-associated
Supernatant
b)
PLA activity [*U*/mg]
1400
1200
1000
800
600
400
200
0
0.46 mg/mL
3.3 mg/mL
PC$_{12:0}$
P. aeruginosa PLs
4
2
0
450
45
4,5
0,45
PaPlaB concentration [ng/ml]
c)
Concentration [µM/OD$_{580nm}$]
200
150
100
50
0
wild-type
Δ*plaB*
*
*
C$_{16:0}$
C$_{17:0}$ cyc(9,10)
C$_{18:0}$
C$_{18:1}$ trans-Δ^{11}
C$_{18:1}$ cis-Δ^{11}
C$_{16:0}$
C$_{17:0}$ cyc(9,10)
C$_{18:0}$
C$_{18:1}$ trans-Δ^{11}
C$_{18:1}$ cis-Δ^{11}
cells
supernatant

Figure 6

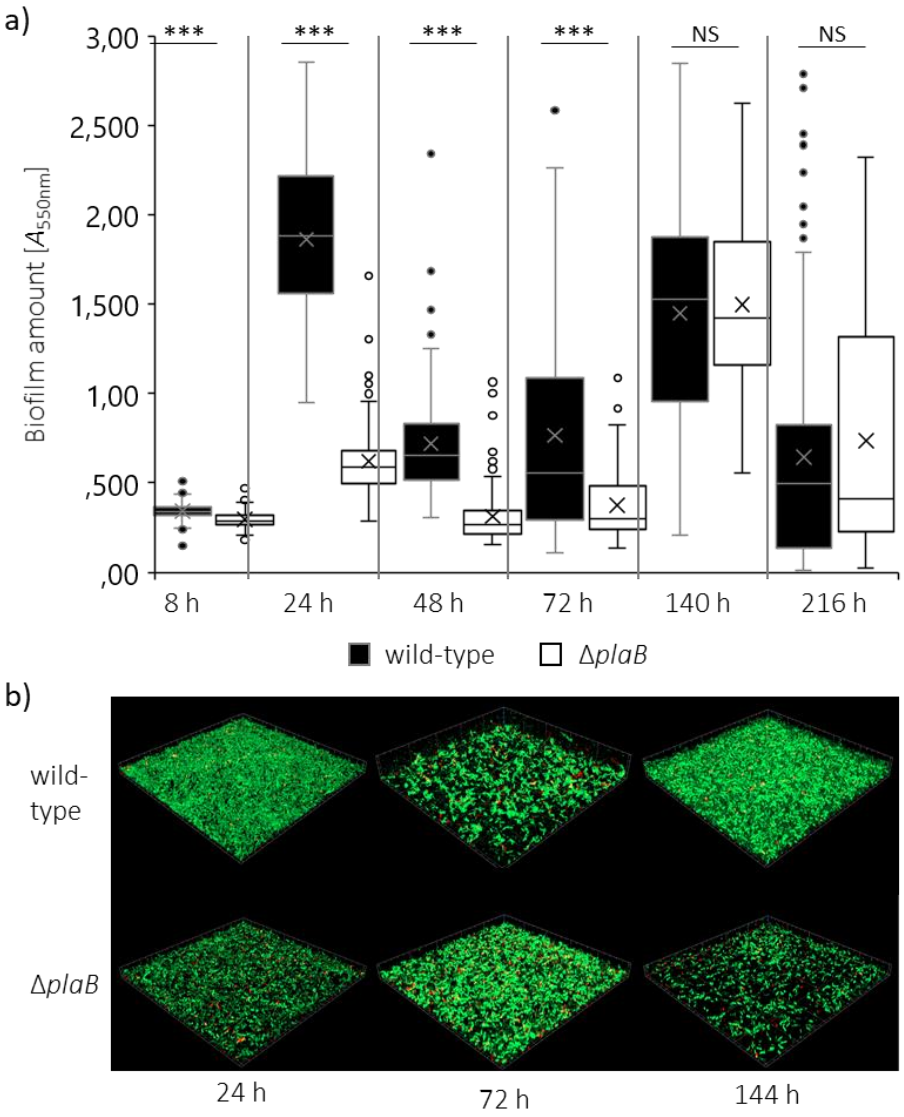
a)
***
***
***
***
NS
NS
3,00
2,500
2,00
1,500
1,00
,500
,00
Biofilm amount [A_{550nm}]
8 h
24 h
48 h
72 h
140 h
216 h
wild-type
ΔplaB
b)
wild-type
ΔplaB
24 h
72 h
144 h

Figure 7